

1 Thermophilic Lithotrophy and Phototrophy in an Intertidal, Iron-rich, Geothermal Spring

2
3 Lewis M. Ward^{1,2,3*}, Airi Idei⁴, Mayuko Nakagawa^{2,5}, Yuichiro Ueno^{2,5,6}, Woodward W.
4 Fischer³, Shawn E. McGlynn^{2*}
5

6 1. Department of Earth and Planetary Sciences, Harvard University, Cambridge, MA 02138 USA

7 2. Earth-Life Science Institute, Tokyo Institute of Technology, Meguro, Tokyo, 152-8550, Japan

8 3. Division of Geological and Planetary Sciences, California Institute of Technology, Pasadena, CA
9 91125 USA

10 4. Department of Biological Sciences, Tokyo Metropolitan University, Hachioji, Tokyo 192-0397,
11 Japan

12 5. Department of Earth and Planetary Sciences, Tokyo Institute of Technology, Meguro, Tokyo,
13 152-8551, Japan

14 6. Department of Subsurface Geobiological Analysis and Research, Japan Agency for Marine-Earth
15 Science and Technology, Natsushima-cho, Yokosuka 237-0061, Japan

16 **Correspondence:** lewis_ward@fas.harvard.edu or mcglynn@elsi.jp
17

18 Abstract

19 Hydrothermal systems, including terrestrial hot springs, contain diverse and systematic
20 arrays of geochemical conditions that vary over short spatial scales due to progressive interaction
21 between the reducing hydrothermal fluids, the oxygenated atmosphere, and in some cases
22 seawater. At Jinata Onsen, on Shikinejima Island, Japan, an intertidal, anoxic, iron- and
23 hydrogen-rich hot spring mixes with the oxygenated atmosphere and sulfate-rich seawater over
24 short spatial scales, creating an enormous range of redox environments over a distance ~10 m.
25 We characterized the geochemical conditions along the outflow of Jinata Onsen as well as the
26 microbial communities present in biofilms, mats, and mineral crusts along its traverse via 16S
27 amplicon and shotgun metagenomic sequencing. The microbial community changed significantly
28 downstream as temperatures and dissolved iron concentrations dropped and dissolved oxygen
29 rose. Near the spring source, primary productivity appears limited, and is fueled primarily by
30 oxidation of ferrous iron and molecular hydrogen by members of the Zetaproteobacteria and
31 Aquificae, while downstream the microbial community is dominated by oxygenic Cyanobacteria.
32 At Jinata Onsen, Cyanobacteria are abundant and productive even at ferrous iron concentrations
33 of ~150 μ M, which challenges the idea that iron toxicity limited cyanobacterial expansion in the
34 Precambrian oceans. Several novel lineages of Bacteria are also present at Jinata Onsen,
35 including previously uncharacterized members of the Chloroflexi and Caldithrichaeota phyla,
36 positioning Jinata Onsen as a valuable site for future characterization of these clades.

37 Importance

38 High temperatures and reducing conditions allow hot springs to support microbial
39 communities that are very different those elsewhere on the surface of the Earth today; in some
40 ways, these environments and the communities they support can be similar to those that existed
41 on the early Earth and that may exist on other planets. Here, we describe a novel hot spring
42 system where hot, iron-rich but oxygen-poor water flows into the ocean, supporting a range of
43 unique microbial communities. Metagenomic sequencing recovered many novel microbial
44 lineages, including deep-branching and uniquely thermotolerant members of known groups.
45 Comparison of the biological productivity of communities in the upstream part of the hot spring,

46 supported by biological iron and hydrogen oxidizing metabolisms, to downstream microbial
47 mats, supported by oxygenic photosynthesis, provides insight into the potential productivity of
48 life on the early Earth and other planets where oxygenic photosynthesis is not possible.

49

50 **Introduction**

51 A major theme of environmental microbiology has been the enumeration of microbial
52 groups that are capable of exploiting diverse chemical potentials that occur in nature (e.g. Broda
53 1977, Strous et al. 1999, Bryant et al. 2007, Ward et al. 2018a). Hot springs, with their varied
54 chemical compositions, provide reservoirs of novel microbial diversity, where environmental and
55 geochemical conditions select for lineages and metabolisms distinct from other Earth-surface
56 environments (e.g. Eloë-Fadrosh et al. 2016, Beam et al. 2016). In addition to their value as
57 sources of microbial diversity, hot springs also provide valuable test beds for understanding
58 microbial community processes driven by different suites of metabolisms (e.g. Inskeep et al.
59 2005)—this in turn provides a process analog window into biosphere function during early times
60 in Earth history, for example when the O₂ content of surface waters was low or non-existent. In
61 contrast to most surface ecosystems which are fueled almost entirely by oxygenic photosynthesis
62 by plants, algae, and Cyanobacteria (Ward and Shih, in review), hot spring microbial
63 communities are commonly supported by lithotrophic or anoxygenic phototrophic organisms that
64 derive energy and electrons for carbon fixation by oxidizing geologically sourced electron
65 donors such as Fe²⁺, sulfide, and molecular hydrogen (e.g. Kawasumi et al. 1998, Spear et al.
66 2005, Ward et al. 2017a). These communities may therefore provide insight into the function of
67 low-productivity communities on the early Earth, before the Great Oxygenation Event ~2.3
68 billion years ago as oxygenic photosynthesis came to dominate primary productivity thereafter
69 (Kharecha et al. 2005, Canfield et al. 2006, Sleep and Bird 2007, Ward and Shih, in review).

70 Here, we present a geomicrobiological characterization of a novel Precambrian Earth
71 process analog site: Jinata Onsen, on Shikinejima Island, Tokyo Prefecture, Japan. At Jinata hot
72 spring, anoxic, iron-rich hydrothermal fluids feed a subaerial spring that flows into a small bay,
73 and mixes with seawater over the course of a few meters. Over its course the waters transition
74 from low-oxygen, iron-rich conditions analogous to some aspects of the early Proterozoic
75 oceans, toward iron-poor and oxygen-rich conditions typical of modern coastal oceans.
76 Coupled to geochemical measurements, 16S amplicon sequencing and shotgun metagenomic
77 sequencing provide an overview of the microbial community composition along the hot spring
78 transect as well as metagenome-assembled genomes of diverse novel microbial lineages that
79 inhabit these springs.

80

81 **Materials and Methods:**

82 **Geological context and sedimentology of Jinata:**

83 Jinata Onsen is located at 34.318 N, 139.216 E on the island of Shikinejima, Tokyo
84 Prefecture, Japan. Shikinejima is part of the Izu Islands, a chain of volcanic islands that formed
85 in the last few million years along the northern edge of the Izu-Bonin-Mariana Arc (Kaneoka et
86 al. 1970). Shikinejima is formed of Late Paleopleistocene- to-Holocene non-alkaline felsic
87 volcanics and Late-Miocene to Pleistocene non-alkaline pyroclastic volcanic flows (Figure 1).

88 The source water of Jinata Onsen emerges anoxic, iron-rich, and gently bubbling from
89 the spring source (Figure 1, Figure 2). Temperatures at the source are ~62°C. Water emerges into
90 the Source Pool, which has no visible microbial mats or biofilms (Figure 2D). Surfaces are
91 instead coated with a fluffy red precipitate, likely a poorly ordered or short range-ordered ferric

92 iron oxide phase such as ferrihydrite. Flow from the Source appears to be—at least in part—
93 tidally charged, with the highest water levels and flow rates occurring at high tide. At low tide,
94 flow rates drop and the water level of the source pool can drop by decimeters. Downstream, the
95 spring water collects into a series of pools (Pool 1-3) (Figure 2C,E-F), which cool sequentially.
96 Pool 1 contains iron oxides like the Source Pool, but also develops macroscopic microbial
97 streamers that are in iron oxides. Streamers are very fine (mm-scale) and delicate (break apart on
98 contact with forceps) but can reach several centimeters in length. Downstream pools (Pools 2
99 and 3) also mix with seawater during high tide due to wave action, but this seawater influence
100 does not appear to influence the Source or Pool 1. Samples were collected and temperatures were
101 measured at high tide, reflecting the lowest temperatures experienced by microbes in the pools—
102 at low tide, hot spring input is dominant and temperatures rise (observed range at each site in
103 Supplemental Table 1). Subaqueous surfaces in Pools 2 and 3 are covered in thick microbial
104 mats. In Pool 2, the mat is coated in a layer of fluffy iron oxide similar to that in the source pool,
105 with dense microbial mat below (Figure 2E). Pool 3 contains only patchy iron oxides, with
106 mostly exposed microbial mats displaying a finger-like morphology. These “fingers” were 0.5-1
107 cm in diameter and up to ~5 cm long and were closely packed and carpeting surfaces of Pool 3
108 below the high tide line. potentially related to turbulent mixing from wave action during high
109 tide (Figure 2F). The Outflow is the outlet of a channel connecting Pool 2 to the bay. Its
110 hydrology is dominantly marine with small admixtures of inflowing spring water (Figure 2G).

111 Jinata hot spring was visited twice for observation and community DNA sampling in
112 2016 (January and September), and again for observation and gas sampling in October 2017 and
113 April 2018. These visits corresponded to a range of tidal conditions, including a spring low and
114 high tide in September 2016. General features of the spring were consistent across this period
115 (including abundance and distribution of iron minerals and microbial mats), differing primarily
116 in an apparent tidal dependence in flow rate and water level of the spring and the amount of
117 seawater influence on Pool 3. These differences in flow and mixing led to variation in water
118 temperatures of 3-10 °C (Supplemental Table 1). At high tide, flow rate of the spring increases,
119 as does seawater influx to Pool 3. During the spring low tide, the spring flow stagnated and the
120 water level of Source Pool and Pool 1 dropped by decimeters. During less extreme low tides
121 observed on other dates, the spring flow was low but nonzero and the water level of the Source
122 Pool did not drop significantly.

123 **Sample collections:**

124 Five sites were sampled at Jinata Onsen: the Source Pool, Pool 1, Pool 2, Pool 3, and the
125 Outflow (Figure 1, Figure 2). During the first sampling trip in January 2016, two whole
126 community DNA samples were collected from each site for 16S amplicon sequencing. During
127 the second sampling trip, additional DNA was collected from the Source Pool and Pool 2 for
128 shotgun metagenomic sequencing.

129 Samples were collected as mineral scrapings of loosely attached, fluffy iron oxide coating
130 from surfaces and clasts upstream (Source Pool and Pool 1) and as samples of microbial mat
131 downstream (Pools 2 and 3, and Outflow) using sterile forceps and spatulas (~0.25 cm³ of
132 material). Immediately after sampling, cells were lysed and DNA preserved with a Zymo
133 Terralyzer BashingBead Matrix and Xpedition Lysis Buffer. Lysis was achieved by attaching
134 tubes to the blade of a Makita JR101DZ cordless reciprocating saw and operating for 1 minute.
135 Aqueous geochemistry samples consisted of water collected with sterile syringes and filtered
136 through a 0.2 µm filter. Gas samples were collected near sites of ebullition emerging from the

137 bottom of the source pool; collection was done into serum vials by water substitution, and then
138 sealed underwater to prevent contamination by air.

139 **Geochemical analysis:**

140 Dissolved oxygen (DO), pH, and temperature measurements were performed *in situ* using
141 an Extech DO700 8-in-1 Portable Dissolved Oxygen Meter (FLIR Commercial Systems, Inc.,
142 Nashua, NH). Iron concentrations were measured using the ferrozine assay (Stokey 1970)
143 following acidification with 40 mM sulfamic acid to inhibit iron oxidation by O₂ or oxidized
144 nitrogen species (Klueglein and Kappler 2013). Ammonia/ammonium concentrations were
145 measured using a TetraTest NH₃/NH₄⁺ Kit (TetraPond, Blacksburg, VA) following
146 manufacturers instructions but with colorimetry of samples and NH₄Cl standards quantified with
147 a Thermo Scientific Nanodrop 2000c spectrophotometer (Thermo Fisher Scientific, Waltham,
148 MA) at 700 nm to improve sensitivity and accuracy. Anion concentrations were measured via
149 ion chromatography on a Shimadzu Ion Chromatograph (Shimadzu Corp., Kyoto, JP) equipped
150 with a Shodex SI-90 4E anion column (Showa Denko, Tokyo, JP).

151 Presence of H₂ and CH₄ in gas samples was qualitatively determined with a Shimadzu
152 GC-14A gas chromatograph within 12 hours of collection to minimize oxidation of reduced
153 gases. Quantitative gas composition was measured following methods described in Suda et al.
154 2017. In brief, gas samples were analyzed using a gas chromatograph (GC-4000, GL Sciences)
155 equipped with both a pulsed discharge detector (PDD) and a thermal
156 conductivity detector (TCD). The GC was equipped with a ShinCarbon ST packed column (2 m
157 × 2.2 mm ID, 50/80 mesh) connected to a HayeSepo Q packed column (2 m × 2.2 mm ID, 60/80
158 mesh) to separate O₂, N₂, CO₂, and light hydrocarbons. Temperature was held at 40°C for 6
159 minutes before ramping up to 200°C at 20°C/min. This temperature was held for 6 minutes
160 before ramping up to 250°C at 50°C/min before a final hold for 15 minutes. The value of
161 standard errors (SE) were determined by replicate measurement of samples. The detection
162 limit was on the order of 1nmol/cc for H₂ and CH₄.

163 **16S sequencing and analysis:**

164 Following return to the lab, microbial DNA was extracted and purified with a Zymo
165 Soil/Fecal DNA extraction kit. The V4-V5 region of the 16S rRNA gene was amplified from
166 each extract using archaeal and bacterial primers 515F (GTGCCAGCMGCCGCGGTAA) and
167 926R (CCGYCAATYMTTTRAGTTT) (Caporaso et al., 2012). DNA was quantified with a
168 Qubit 3.0 fluorimeter (Life Technologies, Carlsbad, CA) according to manufacturer's
169 instructions following DNA extraction and PCR steps. All samples yielded PCR amplicons when
170 viewed on a gel after initial pre-barcoding PCR (30 cycles). Duplicate PCR reactions were
171 pooled and reconditioned for five cycles with barcoded primers. Samples for sequencing were
172 submitted to Laragen (Culver City, CA) for analysis on an Illumina MiSeq platform. Sequence
173 data were processed using QIIME version 1.8.0 (Caporaso et al., 2010). Raw sequence pairs
174 were joined and quality-trimmed using the default parameters in QIIME. Sequences were
175 clustered into de novo operational taxonomic units (OTUs) with 99% similarity using UCLUST
176 open reference clustering protocol (Edgar, 2010). Then, the most abundant sequence was chosen
177 as representative for each *de novo* OTU (Wang et al., 2007). Taxonomic identification for each
178 representative sequence was assigned using the Silva-115 database (Quast et al., 2013) clustered
179 at separately at 99% and at 97% similarity. Singletons and contaminants (OTUs appearing in the
180 negative control datasets) were removed. 16S sequences were aligned using MAFFT (Katoh et
181 al. 2002) and a phylogeny constructed using FastTree (Price et al. 2010). Alpha diversity was
182 estimated using the Shannon Index (Shannon 1948) and Inverse Simpson metric (1/D) (Simpson

183 1949; Hill 1973). All statistics were calculated using scripts in QIIME and are reported at the
184 99% and 97% OTU similarity levels. Multidimensional scaling (MDS) analyses and plots to
185 evaluate the similarity between different samples and OHK environments were produced in R
186 using the vegan and ggplot2 packages (R Core Team 2014, Oksanen et al. 2016, Wickham
187 2009).

188 **Metagenomic sequencing and analysis:**

189 Following initial characterization via 16S sequencing, four samples were selected for
190 shotgun metagenomic sequencing: JP1-A and JP3-A from the first sampling trip, and JP1L-1 and
191 JP2-1 from the second sampling trip. Purified DNA was submitted to SeqMatic LLC (Fremont,
192 CA) for library preparation and 2x100bp paired-end sequencing via Illumina HiSeq 4000
193 technology. Samples JP1-A and JP3-A shared a single lane with two samples from another
194 project (Ward 2017, Ward et al. 2018a), while JP1L-1 and JP2-1 shared a lane with one sample
195 from another project.

196 Raw sequence reads from all four samples were co-assembled with MegaHit v. 1.02 (Li
197 et al. 2016) and genome bins constructed based on nucleotide composition and differential
198 coverage using MetaBAT (Kang et al. 2015), MaxBin (Wu et al. 2014), and CONCOCT
199 (Alneberg et al. 2013) prior to dereplication and refinement with DAS Tool (Sieber et al. 2018)
200 to produce the final bin set. Genome bins were assessed for completeness and contamination
201 using CheckM (Parks et al. 2014), tRNA sequences found with Aragorn (Laslett and Canback
202 2004), and presence of metabolic pathways of interest predicted with MetaPOAP (Ward et al.
203 2018b). Genes of interest (e.g. coding for ribosomal, photosynthesis, and electron transport
204 proteins) were screened against outlier (e.g. likely contaminant) contigs as determined by
205 CheckM using tetranucleotide, GC, and coding density content. Coverage was extracted using
206 bbmap (Bushnell 2016) and samtools (Li et al. 2009). Genes of interest (e.g. coding for
207 ribosomal, photosynthesis, iron oxidation, and electron transport proteins) were identified from
208 assembled metagenomic data locally with BLAST+ (Camacho et al. 2008), aligned with
209 MUSCLE (Edgar 2004), and alignments manually curated in Jalview (Waterhouse et al. 2009).
210 Phylogenetic trees were calculated using RAxML (Stamakis 2014) on the Cipres science
211 gateway (Miller et al. 2010). Node support for phylogenies was calculated with transfer
212 bootstraps by BOOSTER (Lemoine et al. 2018). Trees were visualized with SeaView (Gouy et
213 al. 2010) and the Interactive Tree of Life viewer (Letunic and Bork 2016). Because sequencing
214 depth of each sample in the full metagenome was uneven, relative abundance of genes of interest
215 between metagenomic datasets was normalized to the coverage of *rpoB* genes in each raw
216 dataset as mapped onto the coassembly. Like the 16S gene, *rpoB* is a highly conserved,
217 vertically-inherited gene useful for taxonomic identification of organisms, but has the added
218 advantage that it is only known to occur as a single copy per genome (Case et al. 2007) and is
219 more readily assembled in metagenomic datasets (e.g. Ward et al. 2018a).

220

221 **Results**

222 **Geochemistry**

223 Geochemical measurements along the flow path of Jinata Onsen revealed a significant
224 shift from hot, low-oxygen, high-iron source water to cooler, more oxygen-rich water with less
225 dissolved iron downstream. Geochemistry measurements of Jinata source water are summarized
226 in Table 1 and Supplemental Table 1, while geochemical gradients along the stream outflow are
227 summarized in Figure 3 and Supplemental Table 2. Source waters were slightly enriched in
228 chloride relative to seawater (~23.2 g/L), depleted in sulfate (~1.63 g/L) but approached seawater

229 concentrations downstream as mixing increased. Water emerging from the source was 62°C,
230 very low in dissolved oxygen (~0.15 mg/l), at pH 5.4, and contained substantial concentrations
231 of dissolved iron (~250 $\mu\text{M Fe}^{2+}$). After emerging from the source pool, the spring water
232 exchanges gases with the air due to mixing associated with water flow and gas ebullition, and
233 DO rose to 1.24 mg/L at the surface of the source pool. As water flows downstream from the
234 source pool, it cools slightly, exchanges gases with the atmosphere, and intermittently mixes
235 with seawater below Pool 1.

236 While there is significant variability in the flow rate from the spring based on tides (and
237 resulting shifts in water level and temperature), the overall geochemistry of the source water and
238 the microbial community appeared largely similar between the January and September 2016.

239 Both H_2 and CH_4 were qualitatively detected in bubbles from the source pool following
240 initial sampling in September 2016. However, during subsequent analyses to quantify the gas
241 composition in October 2017 and April 2018 the gas was determined to contain CO_2 , CH_4 , N_2
242 (Supplemental Table 2). This subsequent non-detection of H_2 may be related to temporal
243 variability in the gas composition at Jinata (e.g. following tidal influence; significant variability
244 was observed in the $\text{CO}_2:\text{N}_2$ ratio between two sampling dates, Supplemental Table 2) or may
245 reflect oxidation of H_2 between sampling and analysis; however, the detection limit of H_2 for
246 these later measurements was ~1 nmol/cc, well above the energetic and ecological limits for
247 hydrogenotrophic metabolisms (e.g. Ji et al. 2017) leaving open the possibility of biologically
248 significant H_2 fluxes at Jinata around the time of sampling. This possibility is supported by
249 observations of high relative abundances of microbes with the capacity for hydrogenotrophy,
250 discussed more below.

251 **Sequencing**

252 16S and metagenomic sequencing of microbial communities at Jinata Onsen revealed a
253 highly diverse community. In total, 16S amplicon sequencing recovered 456,737 sequences from
254 the 10 samples at Jinata (Supplemental Table 3, Supplemental Table 4). Reads per sample ranged
255 from 26,057 Source Pool Sample A to 97,445 for Pool 1 Sample A (median 43,331, mean
256 45,673, and standard deviation 19,568). Assessment of sampling depth was estimated using
257 Good's Coverage (Good 1953). On average, 74% of the microbial community was recovered
258 from Jinata samples at the 99% OTU level based on the Good's Coverage statistic (ranging from
259 54% coverage in the Outflow Sample A to 85% in the Pool 1 Sample A) and 87% at the 97%
260 OTU level (74% for the Outflow Sample A to 94.5% for the Pool 1 Sample B). The incomplete
261 sampling—despite sequencing to relatively high depth (>18000 reads per sample)—probably
262 reflects uneven diversity. Greater than 50% of the reads observed at most sites map to the 10
263 most abundant taxa (Supplemental Table 4). MDS analysis (Supplemental Figure 1)
264 demonstrates that samples from the same site are highly similar, and adjacent sites (e.g. Source
265 and Pool 1, Outflow and Pool 3) show significant similarity. However, there is a significant
266 transition in microbial community diversity between the most distant samples (e.g. Source and
267 Outflow).

268 Shotgun metagenomic sequencing of four samples from Jinata Onsen recovered 121 GB
269 of data, forming a 1.48 Gb coassembly consisting of 1531443 contigs with an N50 of 1494 bp.
270 Nucleotide composition and differential coverage-based binning of the coassembly via multiple
271 methods followed by dereplication and refinement resulted in a final set of 161 medium- or high-
272 quality metagenome-assembled genomes (MAGs) following current standards (i.e. completeness
273 >50% and contamination <10%) (Bowers et al. 2017). These MAGs are from diverse phyla of
274 Bacteria and Archaea (Figure 4); metagenome and MAG statistics with tentative taxonomic

275 assignments for recovered MAGs are available in the Supplementary Information (Supplemental
276 Table 5), while MAGs of particular interest are discussed in depth below and shown in
277 phylogenetic trees alongside reference strains in Figures 5-7.

278

279 Discussion

280 The primary trends at Jinata are the transition from hot, low-oxygen, high-iron source
281 waters to cooler, iron-depleted, oxygen-rich water in downstream regions (Figure 3). Following
282 this geochemical transition is a major shift in the composition and productivity of the microbial
283 community, from a high-temperature, lithotrophic community apparently fueled by iron- and
284 hydrogen-oxidation which produces little biomass (at least in net) upstream, to a lower
285 temperature, oxygenic photosynthesis-fueled community with well-developed, thick microbial
286 mats downstream. This shift in community composition is summarized in Figure 3, with
287 complete diversity data in the Supplementary Information (including OTU counts per samples in
288 Supplemental Table 4). Below, we discuss the overall physiological and taxonomic trends across
289 the spring sites as inferred from diversity and genomic analysis.

290 Iron and hydrogen oxidation

291 The hot spring water emerging at the Source Pool at Jinata contains abundant
292 bioavailable electron donors including dissolved Fe^{2+} and likely H_2 (though measurements of gas
293 content varied, as discussed in Results above) (Table 1). These electron donors appear to fuel
294 productivity and determine the microbial community upstream at the Source Pool and Pool 1,
295 where microbial mats are not well developed. The low accumulation of biomass in upstream
296 regions of Jinata are similar to other microbial ecosystems fueled by iron oxidation (e.g. Oku-
297 Okuhachikurou Onsen, Ward et al. 2017a, Fuschna Spring, Helger et al. 2012, and Jackson
298 Creek, Roden et al 2012), in which lithotrophic communities appear much less productive and
299 capable of accumulating less biomass than communities fueled by oxygenic photosynthesis (such
300 as those in downstream regions at Jinata).

301 The most abundant organisms in the Source Pool are members of the Aquificae family
302 Hydrogenothermaceae. Members of this family of marine thermophilic lithotrophs are capable of
303 both iron and hydrogen oxidation (Takai and Nakagawa 2014) and may be utilizing either Fe^{2+} or
304 H_2 at Jinata. The seventh most abundant OTU in the Source Pool samples is a novel sequence
305 89% similar to a strain of *Persephonella* found in an alkaline hot spring in Papua New Guinea.
306 *Persephonella* is a genus of thermophilic, microaerophilic hydrogen oxidizing bacteria within the
307 Hydrogenothermaceae (Götz et al. 2002); the potential difference in bioenergetics between
308 closely related alkaliphiles in Papua New Guinea and strains living at pH 5.5 at Jinata Onsen
309 may be an interesting target for future research. Despite their abundance as assessed by 16S
310 sequencing (Figure 3), only four partial Aquificae MAGs were recovered from Jinata of which
311 only one (J026) was reasonably complete (~94%). Two Aquificae MAGs recovered Group 1
312 NiFe hydrogenase genes, which may be used in hydrogenotrophy; the absence of hydrogenases
313 from the other MAGs may be related to their low completeness, or could reflect a utilization of
314 iron or other electron donors and not H_2 in these organisms.

315 The other most abundant organisms near the source are members of the
316 Zetaproteobacteria—a group typified by the neutrophilic, aerobic iron-oxidizing genus
317 *Mariprofundus* common in marine systems (Emerson et al. 2007). Zetaproteobacteria and
318 Hydrogenothermaceae together made up ~30-65% of 16S sequences in the Source Pool and Pool
319 1, and so appear to drive the base of ecosystem productivity in these upstream pools.

320 The relative abundance of Hydrogenothermaceae drops off to less than 1% of sequences
321 where microbial mats become well developed downstream of Pool 1, but Zetaproteobacteria
322 continue to make up a few percent of reads in Pool 2 and Pool 3 where dissolved iron
323 concentrations are still significant (Figure 3). This suggests that shifts in the relative abundance
324 of may be due more to the increase in abundance of other organisms, rather than a drop in the
325 number of Zetaproteobacteria or their ability to make a living oxidizing iron. In contrast, the
326 absence of Hydrogenothermaceae downstream may be a real signal driven by the rapid
327 disappearance of H₂ as an electron donor. However, in both cases, a drop in relative abundance is
328 likely related to the increasing total biomass (i.e. number of cells) downstream as Cyanobacteria
329 become more productive, leading to sequences from Hydrogenothermaceae and
330 Zetaproteobacteria being swamped out by increases numbers of Cyanobacteria, Chloroflexi, and
331 other sequences. This provides an indirect proxy for the relative productivity of lithotrophs
332 versus oxygenic phototrophs in this environment.

333 Members of the Mariprofundaceae have been observed to have an upper temperature
334 limit for growth of 30°C (Emerson et al. 2010). The Zetaproteobacteria found at Jinata thrive at
335 temperatures up to 63 degrees. This currently represents a unique high-temperature environment
336 for these organisms. In particular, the third most abundant out in the Source Pool and Pool 1
337 sample A is an unknown sequence that is 92% identical to a sequence from an uncultured
338 zetaproteobacterium from a shallow hydrothermal vent in Papua New Guinea (Meyer-Dombard
339 et al. 2013). This sequence likely marks a novel lineage of high-temperature iron-oxidizing
340 Zetaproteobacteria. Four MAGs affiliated with the Zetaproteobacteria were recovered from
341 Jinata with completeness estimates by CheckM ranging from ~80 to ~97% (J005, J009, J030,
342 and J098). While these MAGs did not recover 16S genes, RpoB- and concatenated ribosomal
343 protein-based phylogenies illustrated that members of this group at Jinata Onsen do not belong to
344 the characterized genera *Mariprofundus* or *Ghiorsea*, but instead form separate basal lineages
345 within the Zetaproteobacteria (Figure 5). Despite their phylogenetic distinctness, these MAGs
346 largely recovered genes associated with aerobic iron oxidation, including a terminal O₂ reductase
347 from the C-family of Heme Copper Oxidoreductases for respiration at low O₂ concentrations and
348 C_{yc2} cytochrome genes implicated in ferrous iron oxidation in Zetaproteobacteria and other taxa
349 (e.g. Chlorobi) (Han et al. 2011, Kato et al. 2015, He et al. 2017). Hydrogenase catalytic
350 subunit genes were not recovered in zetaproteobacterial MAGs even at high completeness,
351 suggesting that these organisms are not hydrogenotrophic, though the possibility of
352 uncharacterized hydrogenases cannot be discarded. J098 did not recover a C_{yc2} cytochrome
353 gene; based on phylogenetic position this MAG captures a member of the most basal
354 Zetaproteobacteria lineage recovered to date, which if correct may have diverged prior to the
355 evolution of iron oxidation in this group. However, this MAG is also only 80% complete and so
356 there is a significant probability of failure to recover this gene even if it were present in the
357 source genome (MetaPOAP False Negative estimate 0.205). J005 and J030 did not recover genes
358 for carbon fixation via the Calvin cycle such as the large and small subunits of rubisco,
359 phosphoribulose kinase, or carboxysome proteins; the high completeness of these MAGs (~94-
360 97%) makes it incredibly unlikely that these genes would all fail to be recovered (MetaPOAP
361 False Negative estimates 10⁻⁵-10⁻⁷), suggesting that these strains may be heterotrophic or rely
362 upon an alternative carbon fixation pathway. Over all, the genetic and apparent physiological
363 novelty of Jinata Zetaproteobacteria, along with the site's ease of access relative to typical deep
364 marine settings, makes this a promising target for future isolation and detailed characterization of
365 these taxa.

366 Seven MAGs were recovered from the enigmatic phylum Calditrichaeota (J004, J008,
367 J042, and J075) (Figure 6). Calditrichaeota is a phylum of bacteria with few isolated or
368 sequenced members. The best known of these is *Caldithrix abyssi* (Miroshnichenko et al. 2003);
369 this taxon was characterized as an anaerobic thermophile capable of lithoheterotrophy H₂
370 oxidation coupled to denitrification and organoheterotrophic fermentation (Alauzet and Jumas-
371 Bilak 2014, Marshall et al. 2017). The Calditrichaeota MAGs reported here are up to 97%
372 complete (J004) and contain members with variable metabolic capabilities. Aerobic respiration
373 via A-family Heme Copper Oxidoreductases could potentially be coupled to autotrophic
374 hydrogen oxidation (via the Group 1d NiFe hydrogenase in J042) or iron oxidation (via the *piaA*
375 gene in J075); however, *Caldithrix abyssi* appears incapable of aerobic respiration despite
376 encoding an A-family Heme Copper Oxidoreductase (Kublanov et al. 2017). Unlike previously
377 described Calditrichaeota which are all heterotrophic (Marshall et al. 2017), most of the
378 Calditrichaeota MAGs reported here possess the capacity for carbon fixation via the Calvin
379 cycle. J004 is closely related to *Caldithrix abyssi*, while the other MAGs form two distinct but
380 related clades (Figure 6). These MAGs significantly expand the known genetic and metabolic
381 diversity of this under characterized phylum, and Jinata Onsen may serve as a valuable resource
382 for further research on the physiology and ecology of the Calditrichaeota phylum.

383 The abundance at Jinata of microbes with the genetic capacity for hydrogenotrophy
384 suggests that H₂ may be contributing to lithoautotrophy near the hot spring source, despite H₂
385 concentrations being low (below the detection of ~1 nmol/cc in the gas phase of our quantitative
386 gas analyses, or ~1 nM in the aqueous phase, Amend and Shock 2001). However, this is
387 unsurprising, as the oxidation of H₂ coupled to O₂ reduction is an incredibly thermodynamically
388 favorable process even at vanishingly low substrate concentrations (e.g. $\Delta_r G' < -340$ kJ/mol
389 under conditions at Jinata with substrate concentrations at our limit of detection, Flamholtz et al.
390 2012). Consistent with this thermodynamic favorability, biology has been shown to make use of
391 this metabolism in environments such as hot springs with H₂ concentrations near our detection
392 limits (D'Imperio et al. 2008) and in Antarctic soils where microbes rely on uptake of trace
393 atmospheric H₂ at concentrations around 190 ppbv (Ji et al. 2017). Improved quantification of H₂
394 concentrations and measurement of hydrogenase activity and the productivity of
395 hydrogenotrophic microbes will be needed in future to determine the relative contribution of
396 hydrogen oxidation to productivity at Jinata.

397

398 **Oxygenic photosynthesis**

399 Cyanobacteria are nearly absent from near the source pool, but begin to appear around
400 Pool 1 and become dominant starting in Pool 2. The most abundant Cyanobacteria present are
401 predominantly members of Subsection III, Family I. This group includes *Leptolyngbya*, a genus
402 of filamentous non-heterocystous Cyanobacteria that has appeared in other hot springs of similar
403 temperatures (e.g. Ward et al. 2017a, Roeselers et al. 2007, Bosak et al. 2012). Diverse
404 cyanobacterial MAGs were recovered, including members of the orders Pleurocapsales (J083),
405 Chroococcales (J003 and J149), and Oscillatoriales (J007, J055, and J069).

406 Cyanobacteria performing oxygenic photosynthesis appear to dominate primary
407 productivity in downstream regions of the hot spring, and the filamentous morphology of the
408 strains present here allow them to contribute to the cohesive fabric of the microbial mat.

409 In the outflow samples, chloroplast sequences become abundant, most closely related to
410 the diatom *Melosira*. Algae are at very low abundance upstream of the Out Flow, potentially
411 inhibited by high temperatures, high iron concentrations, ecological competition, or other

412 characteristics of the hot spring water, but the higher seawater influence at the Out Flow appears
413 to create a more permissive environment.

414 Cyanobacteria are sometimes underrepresented in iTag datasets as a result of poor DNA
415 yield or amplification biases (e.g. Parada et al. 2015, Trembath-Reichert et al. 2016), but the low
416 abundance of Cyanobacteria near the Source Pool was confirmed by fluorescent microscopy, in
417 which cells displaying cyanobacterial autofluorescence were observed abundantly in samples
418 from the downstream samples but not in the Source Pool (Supplemental Figure 2).

419 Thick microbial mats, and large accumulations of organic carbon, first appear in Pool 2
420 when Cyanobacteria become abundant. This appears to be related to the high productivity of
421 oxygenic photosynthesis relative to lithotrophic metabolisms (e.g. Ward et al. 2017a, Ward et al.
422 2018c). Consistent with expectations of the nitrogen demand of highly productive oxygenic
423 phototrophic ecosystems relative to poorly productive lithotrophic systems, the abundance of
424 genes for biological nitrogen fixation via nitrogenase was 2.5 times higher in Pool 2 and Pool 3
425 than near the source (*nifD/rpoB* of 0.075 versus 0.03).

426 Previously, it has been suggested that high ferrous iron concentrations are toxic to
427 Cyanobacteria, and that this would have greatly reduced their productivity under ferruginous
428 ocean conditions such as those that may have persisted through much of the Archean era
429 (Swanner et al. 2015). The high cyanobacterial productivity observed at Jinata under high iron
430 concentrations suggest that Cyanobacteria can adapt to ferruginous conditions, and therefore iron
431 toxicity might not inhibit Cyanobacteria over geological timescales. Indeed, the soluble iron
432 concentrations observed at Jinata are higher (150-250 μM) than predicted for the Archean oceans
433 ($<120 \mu\text{M}$, Holland 1984) or observed at other iron-rich hot springs ($\sim 100\text{-}200 \mu\text{M}$, Pierson et al.
434 1999, Ward et al. 2017a), making Jinata an excellent test case for determining the ability of
435 Cyanobacteria to adapt to high iron concentrations. Culture-based physiological experiments
436 may be useful to determine whether Jinata Cyanobacteria utilize similar strategies to other iron-
437 tolerant strains (e.g. the *Leptolyngbya*-relative *Marsacia ferruginosa*, Brown et al. 2010) or
438 whether Jinata strains possess unique adaptations that allow them to grow at higher iron
439 concentrations than known for other environmental Cyanobacteria strains. This will in turn
440 provide insight into whether iron tolerance is due to evolutionarily conserved strategies or
441 whether this is a trait that has evolved convergently multiple times.

442

443 **Diverse novel Chloroflexi from Jinata Onsen**

444 In addition to the primary phototrophic and lithotrophic carbon fixers at Jinata, 16S and
445 metagenomic data sets revealed diverse novel lineages within the Chloroflexi phylum. A total of
446 23 Chloroflexi MAGs were recovered, introducing substantial genetic and metabolic diversity
447 that expands our understanding of this group. While the best known members of this phylum are
448 Type 2 Reaction Center-containing lineages such as *Chloroflexus* and *Roseiflexus* within the
449 class Chloroflexia (e.g. Thiel et al. 2018), phototrophy is not a synapomorphy of the Chloroflexi
450 phylum or even the Chloroflexia class (e.g. Ward et al. 2015a) and most of the diversity of the
451 phylum belongs to several other classes made up primarily of nonphototrophic lineages (Ward et
452 al. 2018a). The bulk of Chloroflexi diversity recovered from Jinata belongs to “Subphylum I”, a
453 broad group of predominantly nonphototrophic lineages that was originally described based on
454 the classes Anaerolineae and Caldilineae (Yamada and Sekiguchi 2009), but also encompasses
455 the related classes Ardenticatenia, Thermoflexia, and *Candidatus Thermofonsia* (Kawaichi et al.
456 2013, Dodsworth et al. 2014, Ward et al. 2018a).

457 16S analysis indicates that members of the Chloroflexi class Anaerolineae are common
458 throughout Jinata with the exception of the Outflow (average 3.5% relative abundance). The
459 Anaerolineae have generally been isolated as obligately anaerobic heterotrophs (e.g. Sekiguchi et
460 al. 2003, Yamada et al. 2006), but genome sequencing of isolates and MAG data from a range of
461 environments has revealed the capacity for aerobic respiration across members of this clade (e.g.
462 Hemp et al. 2015ab, Pace et al. 2015, Ward et al. 2015b, Ward et al. 2018f). It is also likely that
463 a large fraction of 16S sequences annotated as Anaerolineae at Jinata Onsen belong to the sister
464 class *Candidatus* Thermofonsia (Ward et al. 2018a). Three Anaerolineae MAGs were recovered
465 from Jinata (J082, J097, and J130), as compared to seven associated with *Ca.* Thermofonsia
466 (J027, J033, J036, J038, J039, J064, and J076). MAG J036 is an improved version of the genome
467 previously reported as JP3_7 (Ward et al. 2018a), a close relative of *Ca.* *Roseilinea gracile* (Klatt
468 et al. 2011, Tank et al. 2017, Thiel et al. 2017). J036 contains a 16S gene that is 96% similar to
469 that of *Ca.* *Roseilinea gracile*, and thus these strains are probably best classified as distinct
470 species within the same genus. Unlike other phototrophs in the Chloroflexi phylum that are
471 capable of photoautotrophy via the 3-hydroxypropionate bicycle or the Calvin Cycle (Klatt et al.
472 2007, Shih et al. 2017), J036 and *Ca.* *Roseilinea gracile* do not encode carbon fixation and are
473 likely photoheterotrophic. Previous analyses suggested that the *Roseilinea* lineage belongs to the
474 Anaerolineae (Klatt et al. 2011) or Thermofonsia (Ward et al. 2018a) classes; however, our
475 updated phylogeny presented here places J036 and *Roseilinea* in a separate lineage along with
476 J033 and J162, diverging just outside of the Anaerolineae+Thermofonsia clade, suggesting that
477 these strains may instead be yet another class-level lineage within the broader “Subphylum I” of
478 Chloroflexi (Figure 7).

479 Members of the Chloroflexi class Caldilineae were present at up to ~1% abundance at
480 Jinata in the 16S dataset. Members of the Caldilineae have previously been isolated from
481 intertidal hot springs in Iceland (Kale et al. 2013) and Japanese hot springs (Sekiguchi et al.
482 2003). Characterized organisms in this class are filamentous, anaerobic, or facultatively aerobic
483 heterotrophs (Sekiguchi et al. 2003, Grégoire et al. 2011, Kale et al. 2013); and therefore these
484 taxa may play a role in degrading biomass within low-oxygen regions of microbial mats. Several
485 MAGs from within the Caldilineae and related lineages were recovered in the metagenome,
486 potentially reflecting novel class-level diversity within the Chloroflexi. Three MAGs were
487 recovered that form a clade sister to the previously characterized members of the Caldilineae
488 class *Caldilinea* and *Litorilinea* (J095, J111, and J123), forming a deeply branching lineage
489 within this class. Like other members of the Caldilineae, these strains encode aerobic respiration
490 via a family Heme Copper Oxidoreductases and both a *bc* complex III and an Alternative
491 Complex III, and are therefore likely at least facultatively aerobic. J095 also encodes carbon
492 fixation via the Calvin cycle as well as a Group 1f NiFe hydrogenase, suggesting a potential
493 capability for lithoautotrophy by hydrogen oxidation, expanding the known metabolic diversity
494 of this class and the Chloroflexi phylum as a whole.

495 The Chloroflexi class Ardenticatena was first described from an isolate from an iron-rich
496 Japanese hydrothermal field (Kawaichi et al. 2013) and has since been recovered from sulfidic
497 hot springs as well (Ward et al. 2018e). A MAG closely related to *Ardenticatena maritima* was
498 recovered from Jinata Onsen, J129. While *Ardenticatena maritima* 110S contains a complete
499 denitrification pathway (Hemp et al. 2015), MAG J129 did not recover any denitrification genes.
500 This could be related to the relatively low completeness of this MAG (~70%), but False Negative
501 estimates by MetaPOAP (Ward et al. 2018c) indicates that the probability that all four steps in
502 the canonical denitrification pathway would fail to be recovered in J129 given their presence in the

503 source genome is less than 0.8%, suggesting that most if not all denitrification genes are truly
504 absent and that the capacity for denitrification is not universal within members of *Ardenticatena*.
505 This would be consistent with broad trends in the apparently frequent modular horizontal gene
506 transfer of partial denitrification pathways between disparate microbial lineages to drive rapid
507 adaption and metabolic flexibility of aerobic organisms in microoxic and anoxic environments,
508 for reasons that are still not well established (Chen and Strous 2013, Stein and Klotz 2016).

509 MAG J114 branches at the base of Subphylum I of the Chloroflexi, potentially the first
510 member of a novel class-level lineage. The divergence between Anaerolineae and Caldilineae
511 has been estimated to have occurred on the order of 1.7 billion years ago (Shih et al. 2017). The
512 phylogenetic placement of J114 suggests that it diverged from other members of Subphylum I
513 even earlier, and it may be a good target for future investigation to assess aspects of the early
514 evolution of the Chloroflexi phylum. J114 encodes aerobic respiration via an A family Heme
515 Copper Oxidoreductase and an Alternative Complex III like many other nonphototrophic
516 Chloroflexi lineages (e.g. Ward et al. 2015a, Ward et al. 2018a) as well as a Group 1f NiFe
517 hydrogenase and carbon fixation via the Calvin Cycle, suggesting the capacity for aerobic
518 hydrogen-oxidizing autotrophy—a lifestyle not previously described for members of the
519 Chloroflexi. The Alternative Complex III encoded by J114 branches basally to a clade of ACIII
520 sequences from other Subphylum I Chloroflexi, potentially reflecting vertical inheritance of
521 ACIII from the last common ancestor of this clade; however, the A-family Heme Copper
522 Oxidoreductase encoded by J114 is in a more derived position closely related to sequences from
523 members of the Caldilineae, and may have been acquired via horizontal gene transfer from a
524 member of this group.

525

526 **Conclusions**

527 Jinata Onsen is a environment supporting especially strong geochemical gradients over
528 short spatial scales. The transition from low-oxygen, iron- and hydrogen-rich hot spring source
529 water to oxygen-rich ocean water takes place over just a few meters, and results in an almost
530 complete change in microbial community. We have recovered substantial genetic and metabolic
531 novelty from metagenomic data from Jinata Onsen, highlighting how hot spring microbial
532 communities (particularly those of understudied iron-rich systems) are hotbeds of poorly
533 characterized microbial clades. In addition, due to its utility as an environment to investigate the
534 diversity and ecology of microbes, including thermal tolerant iron-oxidizing Zetaproteobacteria
535 and iron-tolerant Cyanobacteria, this system is significant for its relevance as a process analog
536 for environments through Earth history and potentially habitable environments in Mars' past.

537 The diversity of iron oxidizing bacteria at Jinata is very different than in other Fe²⁺-rich
538 springs and environments. For example, in freshwater systems such as Oku-Okuhachikurou
539 Onsen in Akita Prefecture, Japan (Ward et al. 2017), and Budo Pond in Hiroshima, Japan (Kato
540 et al. 2012), iron oxidation is driven primarily by the activity of chemoautotrophs such as
541 members of the Gallionellaceae (Ward et al. 2017). In contrast, at Chocolate Pots hot spring in
542 Yellowstone National Park, USA, iron oxidation is primarily abiotic, driven by O₂ produced by
543 Cyanobacteria, with only a small contribution from iron oxidizing bacteria (Trouwborst et al.
544 2007, Fortney et al. 2018). The distinct iron-oxidizing community at Jinata Onsen may be related
545 to the salinity of the spring water, or biogeographically by access to the ocean, as
546 Zetaproteobacteria are typically found in marine settings, particularly in deep ocean basins
547 associated with hydrothermal iron sources (Emerson et al. 2010). Despite the taxonomically
548 distinct iron oxidizer communities between Jinata and Oku-Okuhachikurou Onsen, both

549 communities support only limited biomass in regions dominated by iron oxidizers (Ward et al.
550 2017a), perhaps reflecting the shared biochemical and bioenergetic challenges iron oxidation
551 incurred by diverse iron oxidizing bacteria including Gallionellaceae and Zetaproteobacteria
552 (Emerson et al. 2010, Bird et al. 2011, Ward et al. 2017a).

553 Throughout Earth history, the metabolic opportunities available to life, and the resulting
554 organisms and metabolisms responsible for driving primary productivity, have been shaped by
555 the geochemical conditions of the atmosphere and oceans. Over the course of Earth's four-and-a-
556 half billion-year history, the redox state and overall geochemical conditions of the oceans have
557 varied systematically. The modern, sulfate-rich, well-oxygenated oceans we see today reflects a
558 relatively recent state—one typical of only the last few hundred million years (e.g. Lyons et al.
559 2014). For the first half of Earth history, until ~2.3 billion years ago (Ga), the atmosphere and
560 oceans were anoxic (Johnson et al. 2014), and the oceans were largely rich in dissolved iron but
561 poor in sulfur (Walker and Brimblecombe 1985). At this time, productivity was low and fueled
562 by metabolisms such as methanogenesis and anoxygenic photosynthesis (Kharecha et al. 2005,
563 Canfield et al. 2006, Ward et al. 2018c). Following the expansion of oxygenic photosynthesis by
564 Cyanobacteria and higher primary productivity around the Great Oxygenation Event ~2.3 Ga
565 (Fischer et al. 2016, Ward et al. 2016, Crockford et al. 2018, Ward et al. 2018c), the atmosphere
566 and surface ocean accumulated some oxygen, and the ocean transitioned into a state with
567 oxygenated surface waters but often anoxic deeper waters, rich in either dissolved iron or sulfide
568 (Canfield 1998, Poulton et al. 2010, Johnston et al. 2009, Johnston et al. 2010). Many individual
569 environments have been characterized that are interpreted to be analogous to a particular period
570 in Earth history; these include Lake Matano, in Indonesia, interpreted as being analogous to the
571 ferruginous ocean (Crowe et al. 2008), Oku-Okuhachikurou Onsen in Akita Prefecture, Japan,
572 similar to conditions just following the GOE (Takashima et al. 2011, Ward et al. 2017a), and
573 Lake Cadagno in Switzerland and the Black Sea, analogous to conditions hypothesized for
574 euxinic Proterozoic oceans (Canfield et al. 2010, Scott et al. 2008). These analogs are each
575 valuable in their own right, but the major differences in context at each site makes it difficult to
576 isolate individual variables that lead to shifts in microbial community and productivity.

577 At Jinata Onsen, this range of geochemical conditions is recapitulated over just a few
578 meters, providing a useful test case for probing the shifts of microbial productivity over the
579 course of Earth history as conditions vary over short spatial scales. In particular, the concomitant
580 increase in net primary production at Jinata as the community shifts from lithotrophy toward
581 water-oxidizing phototrophy (i.e. oxygenic photosynthesis) is consistent with estimates for
582 greatly increased primary production following the evolution of Cyanobacteria around the GOE
583 (Sleep and Bird 2007, Ward et al. 2016, Ward et al. 2017a, Crockford et al. 2018, Ward et al.
584 2018c, Ward and Shih 2018).

585 The dynamic abundances of redox-active compounds including oxygen, iron, and
586 hydrogen at Jinata may not only be analogous to conditions on the early Earth, but may have
587 relevance for potentially habitable environments on Mars as well. Early Mars is thought to have
588 supported environments with metabolic opportunities provided by the redox gradient between
589 the oxidizing atmosphere and abundant electron donors such as ferrous iron and molecular
590 hydrogen sourced from water/rock interactions (e.g. Hurowitz et al. 2010), and production of
591 these substrates may continue today (Stamenkovic et al. 2018, Dzaugis et al. 2018).
592 Understanding the potential productivity of microbial communities fueled by lithotrophic
593 metabolisms is critical for setting expectations of the presence and size of potential biospheres on
594 other worlds and early in Earth history (e.g. Ward et al. 2017a, Ward 2017, Ward et al. 2018d).

595 Uncovering the range of microbial metabolisms present under the environmental conditions at
596 Jinata, and their relative contributions to primary productivity, may therefore find application to
597 predicting environments on Mars most able to support productive microbial communities.

598

599 **Data availability:**

600 Raw 16S and metagenomic sequence data have been uploaded to the Sequence Read Archive
601 (Submission #SUB4558398) and MAGs have been uploaded to Genbank (Submission
602 #SUB4557661). All data will be made publicly available immediately following processing.

603

604 **Figure 1:**

605 Location of Jinata Onsen on Shikinejima Island, Japan, and inset overview sketch of field site
606 with sampling localities marked.

607

608 **Figure 2:**

609 Representative photos of Jinata. A) Panorama of field site, with source pool on left (Pool 1
610 below), Pool 2 and 3 in center, and Out Flow to bay on right. B) Undistorted view north up the
611 canyon. C) Undistorted view south toward bay, overlooking Pool 2. D) Source pool, coated in
612 flocculent iron oxides and bubbling with gas mixture containing H₂, CO₂, and CH₄. E) Pool 2, with
613 mixture of red iron oxides and green from Cyanobacteria-rich microbial mats. F) Close up of
614 textured microbial mats in Pool 3. G) Close up of Out Flow, where hot spring water mixes with
615 ocean water.

616

T	63°C
pH	5.4
DO	4.7 μM
Fe²⁺	261 μM
NH₃/NH₄⁺	87 μM
Cl⁻	654 mM
SO₄²⁻	17 mM
NO₃⁻	<1.6 μM
NO₂⁻	<2.2 μM
HPO₄⁻	<1 μM

617 **Table 1:** Geochemistry of source water at Jinata Onsen.

618

619 **Figure 3:**

620 Summary of geochemical and microbiological trends along the flow path of Jinata Onsen. Top:
621 panoramic view of Jinata Onsen, with source pool at left and flow of spring water toward the bay
622 at right, with sampling locations indicated. Middle: geochemical transect across the spring,
623 showing temperature (°C) and dissolved Fe(II) and O₂ (μM). Bottom: stacked bar chart of
624 relative community abundance of dominant microbial phyla as determined by 16S amplicon
625 sequencing. Sequence data were binned at the phylum level averaged at each sample site. Reads
626 that could not be assigned to a phylum were discarded; all phyla that do not make up more than
627 2% of the community at any one site have been collapsed to “Other”. Near the source, the
628 community is predominantly made up of iron- and/or hydrogen-oxidizing organisms in the
629 Proteobacteria and Aquificae phyla. As the hot spring water flows downstream, it equilibrates
630 with the atmosphere and eventually mixes with seawater, resulting in downstream cooling,

631 accumulation of oxygen, and loss of dissolved iron due to biological and abiotic processes.
632 Oxygenic Cyanobacteria become progressively more abundant downstream Hydrogen- and iron-
633 oxidizing lithotrophs dominate near the source, but phototrophic Cyanobacteria come to
634 dominate downstream. Additional community diversity is found Supplemental Table 4.

635
636 **Figure 4:**
637 Phylogeny of Bacteria and Archaea based on concatenated ribosomal proteins. Numbers in
638 parentheses next to phylum labels refer to number of MAGs recovered from Jinata Onsen.
639 Labels for phyla with two or fewer MAGs recovered from Jinata omitted for clarity. Reference
640 alignment modified from Hug et al. 2016. Full list of MAGs recovered available in Supplemental
641 Table 5.

642 **Figure 5:** Phylogeny of the Zetaproteobacteria, rooted with Alphaproteobacteria, built with
643 concatenated ribosomal protein sequences. Data from Singer et al. 2011, Mori et al. 2017,
644 Makita et al. 2017, and other draft genomes available on Genbank. All nodes recovered TBE
645 support values greater than 0.7. In cases where reference genomes have a unique strain name or
646 identifier, this is included; otherwise Genbank WGS genome prefixes are used.

647
648 **Figure 6:** Phylogeny of the Calditrichaeota, rooted with Bacteroidetes, built with concatenated
649 ribosomal protein sequences. Data from Kublanov et al. 2017 and other draft genomes available
650 on genomes have a unique strain name or identifier, this is included; otherwise Genbank WGS
651 genome prefixes are used.

652 **Figure 7:** Detailed phylogeny of the Chloroflexi phylum, with class-level clades highlighted in
653 gray, built with concatenated ribosomal protein sequences. The large basal class
654 Dehalococcoidia, which was not observed in 16S or metagenome data from Jinata, is omitted for
655 clarity. Contains MAGs reported here, members of the Chloroflexi phylum previously described
656 (Chang et al. 2011, Kuznetsov et al. 2011, Sorokin et al. 2012, Kawaichi et al. 2015, Dodsworth
657 et al. 2014, Hedlund et al. 2015, Ward et al. 2015a, Ward et al. 2015b, Hemp et al. 2015a, Hemp
658 et al. 2015b, Hemp et al. 2015c, Pace et al. 2015, Ward 2017, Ward et al. 2018a, Ward et al.
659 2018e, Ward et al. 2018f), and members of the closely related phylum Armatimonadetes as an
660 outgroup (Dunfield et al. 2012, Ward et al. 2017). MAGs described here highlighted in green,
661 MAGs previously reported from Jinata Onsen highlighted in pink. All nodes recovered TBE
662 support values greater than 0.7. In cases where reference genomes have a unique strain name or
663 identifier, this is included; otherwise Genbank WGS genome prefixes are used.

664
665 **Supplemental Figure 1:**
666 Multidimensional scaling plot of Jinata samples. Each point represents the recovered microbial
667 community from a given sample, with sites identified by color and sample type by shape.
668 Samples plotting close to each other are relatively more similar in community composition.
669 Abundance data are transformed by the 4th root to down-weight the effect of abundant taxa.
670 Stress value is 0.0658.

671 **Supplemental Figure 2:**

672 Microscopy images of sediment (Source and Pool 1) or mat (Pool 2, Pool 3, and Out Flow). Left
 673 are light microscopy images. Center and right are fluorescence images. At center, blue signal is
 674 DAPI-stained (Excitation: 365nm, Emission: BP445~50nm). At right, red is autofluorescence
 675 signal of Cyanobacteria (BP395~440nm, LP470nm). Scale bars 50 μ m.

	pH	T (°C)	Fe(II) (μM)	DO (μM)	Descriptions
Source	5.4	60-63	260	4.7 (source) 39 (surface)	Fluffy red iron oxide precipitate
Pool 1	5.8	59-59.5	265	58	Reddish precipitate and streamers in shallower regions, more yellowish deeper
Pool 2	6.5	44.5-54	151	134	Iron oxide-coated microbial mats. Orange to orange-green.
Pool 3	6.7	37.3-46	100	175	Green or mottled orange-green microbial mats, commonly with 1-5cm finger-like morphology.
Outflow	6.5	27-32	45	234	Ocean water within mixing zone at high tide, with constant flow of spring water from Pool 2. Thin green microbial mats.

676 **Supplemental Table 1:** Geochemistry and brief description at sampling sites along the flow path
 677 of Jinata Onsen as discussed in the text.

Sampling dates (mm/dd/yyyy)	Measurement number	Average of gas compositions (percent composition)							
		N ₂	SE	O ₂	SE	CH ₄	SE	CO ₂	SE
10/03/2017	2	30.5	4.6	0.10	0.01	0.04	0.01	69.3	4.6
04/13/2018	4	55.5	5.5	0.07	0.04	0.05	0.01	44.4	5.0

678

679

680 **Supplemental Table 2:** Gas composition of bubbles collected from the Source Pool at Jinata
 681 Onsen.

682

Sample:	Reads:	OTUs (99%):	Good Coverage (99%):	Shannon Index (99%):	Inverse Simpson (99%):	OTUs (97%):	Good Coverage (97%):	Shannon Index (97%):	Inverse Simpson (97%):
Source A	26057	95 58	0.724	10.594	83.020	4632	0.884	8.196	23.035
Source B	49340	14 39	0.790	10.275	44.714	5530	0.932	7.229	12.835

		2							
		21							
		16							
Pool 1 A	97445	6	0.848	10.128	56.287	10160	0.935	8.080	24.682
		10							
		55							
Pool 1 B	57250	9	0.872	8.794	33.323	4766	0.945	6.414	12.005
		13							
		11							
Pool 2 A	41515	4	0.759	9.754	24.340	7710	0.873	8.118	14.702
		17							
		21							
Pool 2 B	45171	1	0.697	10.708	50.836	10525	0.832	8.980	25.783
		15							
		98							
Pool 3 A	45148	8	0.722	10.287	33.295	9302	0.853	8.351	16.880
		12							
		02							
Pool 3 B	29778	3	0.682	10.894	84.725	6625	0.837	8.553	31.520
		17							
		74							
Outflow A	32382	1	0.542	11.931	57.572	11290	0.738	10.262	28.674
		88							
Outflow B	32651	81	0.797	9.237	28.728	4210	0.909	6.373	9.850

683 **Supplemental Table 3:**

684 Diversity metrics of Jinata sequencing. Diversity metrics calculated for both 99% and 97%
685 sequence identity cutoffs for assigning OTUs.

686

687 **Supplemental Table 4:**

688 16S data as OTU table with sequences.

689

690 **Supplemental Table 5:**

691 High- and medium-quality metagenome-assembled genomes (MAGs) (>50% completeness and
692 <10% contamination) recovered from Jinata Onsen.

693

694 **References**

- 695 1. Alauzet, C., & Jumas-Bilak, E. (2014). The phylum Deferribacteres and the genus *Caldithrix*.
696 In *The Prokaryotes*(pp. 595-611). Springer Berlin Heidelberg.
- 697 2. Alneberg, J., Bjarnason, B. S., de Bruijn, I., Schirmer, M., Quick, J., Ijaz, U. Z., ... & Quince,
698 C. (2013). CONCOCT: clustering contigs on coverage and composition. *arXiv preprint*
699 *arXiv:1312.4038*.
- 700 3. Amend, J. P., & Shock, E. L. (2001). Energetics of overall metabolic reactions of
701 thermophilic and hyperthermophilic Archaea and Bacteria. *FEMS microbiology*
702 *reviews*, 25(2), 175-243.
- 703 4. Anbar, a D. & Knoll, a H. Proterozoic ocean chemistry and evolution: a bioinorganic bridge?
704 *Science* **297**, 1137–1142 (2002).

- 705 5. Baldani, José Ivo, et al. "The family rhodospirillaceae." *The Prokaryotes*. Springer Berlin
706 Heidelberg, 2014. 533-618.
- 707 6. Barns, Susan M., Shannon L. Takala, and Cheryl R. Kuske. "Wide distribution and diversity
708 of members of the bacterial kingdom Acidobacterium in the environment." *Applied and
709 environmental microbiology* 65.4 (1999): 1731-1737.
- 710 7. Bird, L. J., Bonnefoy, V. & Newman, D. K. Bioenergetic challenges of microbial iron
711 metabolisms. *Trends Microbiol.* 19, 330–340 (2011).
- 712 8. Bosak, T. et al. Cyanobacterial diversity and activity in modern conical microbialites.
713 *Geobiology* 10, 384–401 (2012).
- 714 9. Brocks, J. J. et al. Biomarker evidence for green and purple sulphur bacteria in a stratified
715 Palaeoproterozoic sea. *Nature* 437, 866–870 (2005).
- 716 10. Broda, E. (1977). Two kinds of lithotrophs missing in nature. *Zeitschrift für allgemeine
717 Mikrobiologie*, 17(6), 491-493.
- 718 11. Brown, Igor I., et al. "Polyphasic characterization of a thermotolerant siderophilic
719 filamentous cyanobacterium that produces intracellular iron deposits." *Applied and
720 environmental microbiology* 76.19 (2010): 6664-6672.
- 721 12. Bushnell, B. "BBMap short read aligner." *University of California, Berkeley, California*.
722 URL <http://sourceforge.net/projects/bbmap> (2016).
- 723 13. Camacho C., Coulouris G., Avagyan V., Ma N., Papadopoulos J., Bealer K., & Madden T.L.
724 (2008) "BLAST+: architecture and applications." *BMC Bioinformatics* 10:421.
- 725 14. Canfield, D. E. (1998). A new model for Proterozoic ocean chemistry. *Nature*, 396(6710),
726 450.
- 727 15. Canfield, D. E., Rosing, M. T. & Bjerrum, C. Early anaerobic metabolisms. *Philos. Trans. R.
728 Soc. B Biol. Sci.* **361**, 1819–1836 (2006).
- 729 16. Canfield, D. E., Farquhar, J., & Zerkle, A. L. (2010). High isotope fractionations during
730 sulfate reduction in a low-sulfate euxinic ocean analog. *Geology*, 38(5), 415-418.
- 731 17. Caporaso, J. G. et al. Ultra-high-throughput microbial community analysis on the Illumina
732 HiSeq and MiSeq platforms. *ISME J* 6, 1621–1624 (2012).
- 733 18. Caporaso, J. Gregory, et al. "QIIME allows analysis of high-throughput community
734 sequencing data." *Nature methods* 7.5 (2010): 335-336.
- 735 19. Case, R. J. *et al.* Use of 16S rRNA and rpoB genes as molecular markers for microbial
736 ecology studies. *Appl. Environ. Microbiol.* **73**, 278–288 (2007).
- 737 20. Castelle, C. J., Wrighton, K. C., Thomas, B. C., Hug, L. A., Brown, C. T., Wilkins, M. J., ...
738 & Taylor, R. C. (2015). Genomic expansion of domain archaea highlights roles for
739 organisms from new phyla in anaerobic carbon cycling. *Current biology*, 25(6), 690-701.
- 740 21. Catling, D. C., Glein, C. R., Zahnle, K. J. & McKay, C. P. Why O₂ is required by complex
741 life on habitable planets and the concept of planetary 'oxygenation time'. *Astrobiology* **8**,
742 377–395 (2005).
- 743 22. Chan, Clara S., et al. "Lithotrophic iron-oxidizing bacteria produce organic stalks to control
744 mineral growth: implications for biosignature formation." *The ISME journal* 5.4 (2011): 717-
745 727.
- 746 23. Chan, Clara S., et al. "The architecture of iron microbial mats reflects the adaptation of
747 chemolithotrophic iron oxidation in freshwater and marine environments." *Frontiers in
748 Microbiology* 7 (2016).
- 749 24. Chan, C. S., Emerson, D. & Luther, G. W. The role of microaerophilic Fe-oxidizing micro-
750 organisms in producing banded iron formations. *Geobiology* **14**, 509–528 (2016b).

- 751 25. Chang, Y. J., Land, M., Hauser, L., Chertkov, O., Del Rio, T. G., Nolan, M., ... & Han, C.
752 (2011). Non-contiguous finished genome sequence and contextual data of the filamentous
753 soil bacterium *Ktedonobacter racemifer* type strain (SOSP1-21 T). *Standards in genomic*
754 *sciences*, 5(1), 97.
- 755 26. Chen, J., & Strous, M. (2013). Denitrification and aerobic respiration, hybrid electron
756 transport chains and co-evolution. *Biochimica et Biophysica Acta (BBA)-*
757 *Bioenergetics*, 1827(2), 136-144.
- 758 27. Crockford, P. W., Hayles, J. A., Bao, H., Planavsky, N. J., Bekker, A., Fralick, P. W., ... &
759 Wing, B. A. (2018). Triple oxygen isotope evidence for limited mid-Proterozoic primary
760 productivity. *Nature*, 559(7715), 613.
- 761 28. Crowe, S. A. et al. Photoferrotrophs thrive in an Archean Ocean analogue. *Proc. Natl. Acad.*
762 *Sci.* 105, 15938–15943 (2008).
- 763 29. Daims, Holger. "The family nitrospiraceae." *The Prokaryotes*. Springer Berlin Heidelberg,
764 2014. 733-749.
- 765 30. D'Imperio, S., Lehr, C. R., Oduro, H., Druschel, G., Köhl, M., & McDermott, T. R. (2008).
766 Relative importance of H₂ and H₂S as energy sources for primary production in geothermal
767 springs. *Applied and environmental microbiology*, 74(18), 5802-5808.
- 768 31. Dodsworth, J. A., Gevorkian, J., Despujos, F., Cole, J. K., Murugapiran, S. K., Ming, H., ...
769 & Hedlund, B. P. (2014). *Thermoflexus hugenholtzii* gen. nov., sp. nov., a thermophilic,
770 microaerophilic, filamentous bacterium representing a novel class in the Chloroflexi,
771 *Thermoflexia* classis nov., and description of *Thermoflexaceae* fam. nov. and *Thermoflexales*
772 *ord. nov.* *International journal of systematic and evolutionary microbiology*, 64(6), 2119-
773 2127.
- 774 32. Dunfield, P. F., Tamas, I., Lee, K. C., Morgan, X. C., McDonald, I. R., & Stott, M. B.
775 (2012). Electing a candidate: a speculative history of the bacterial phylum
776 OP10. *Environmental microbiology*, 14(12), 3069-3080.
- 777 33. Dzaugis, M., Spivack, A. J., & D'Hondt, S. (2018). Radiolytic H₂ Production in Martian
778 Environments. *Astrobiology*.
- 779 34. Edgar RC. 2010. Search and clustering orders of magnitude faster than
780 BLAST. *Bioinformatics* 26(19):2460-2461.
- 781 35. Ehrenreich, A., and Widdel, F., 1994, Anaerobic oxidation of ferrous iron by purple bacteria,
782 a new type of phototrophic metabolism: *Applied and Environmental Microbiology*, v. 60, p.
783 4517–4526
- 784 36. Emerson, D. *et al.* A novel lineage of proteobacteria involved in formation of marine Fe-
785 oxidizing microbial mat communities. *PLoS One* 2, (2007).
- 786 37. Emerson, D., Fleming, E. J. & McBeth, J. M. Iron-oxidizing bacteria: an environmental and
787 genomic perspective. *Annu. Rev. Microbiol.* 64, 561–583 (2010).
- 788 38. Fischer, W., Hemp, J. & Johnson, J. E. Evolution of Oxygenic Photosynthesis. *Annu. Rev.*
789 *Earth Planet. Sci.* 44, (2016).
- 790 39. Fortney, N. W., He, S., Converse, B. J., Boyd, E. S., & Roden, E. E. (2018). Investigating the
791 Composition and Metabolic Potential of Microbial Communities in Chocolate Pots Hot
792 Springs. *Front. Microbiol.* 9: 2075. doi: 10.3389/fmicb.
- 793 40. Fukunaga, Y. *et al.* *Phycisphaera mikurensis* gen. nov., sp nov., isolated from a marine alga,
794 and proposal of *Phycisphaeraceae* fam. nov., *Phycisphaerales* ord. nov and *Phycisphaerae*
795 *classis nov* in the phylum Planctomycetes. *J. Gen. Appl. Microbiol.* 55, 267–275 (2009).

- 796 41. Garrity, George M., et al. "Phylum BIX. Deferribacteres phy. nov." *Bergey's Manual® of*
797 *Systematic Bacteriology*. Springer New York, 2001. 465-471.
- 798 42. Geider, Richard J., et al. "Primary productivity of planet earth: biological determinants and
799 physical constraints in terrestrial and aquatic habitats." *Global Change Biology* 7.8 (2001):
800 849-882.
- 801 43. GOOD, I.J., 1953, The population frequencies of species and the estimation of population
802 parameters: *Biometrika*, v. 40, p. 237-264.
- 803 44. Götz, D., et al. "Persephonella marina gen. nov., sp. nov. and Persephonella guaymasensis sp.
804 nov., two novel, thermophilic, hydrogen-oxidizing microaerophiles from deep-sea
805 hydrothermal vents." *International Journal of Systematic and Evolutionary*
806 *Microbiology* 52.4 (2002): 1349-1359.
- 807 45. Grégoire, P., Bohli, M., Cayol, J. L., Joseph, M., Guasco, S., Dubourg, K., ... & Ollivier, B.
808 (2011). *Caldilinea tarbellica* sp. nov., a filamentous, thermophilic, anaerobic bacterium
809 isolated from a deep hot aquifer in the Aquitaine Basin. *International journal of systematic*
810 *and evolutionary microbiology*, 61(6), 1436-1441.
- 811 46. Han, H., Hemp, J., Pace, L. A., Ouyang, H., Ganesan, K., Roh, J. H., ... & Gennis, R. B.
812 (2011). Adaptation of aerobic respiration to low O₂ environments. *Proceedings of the*
813 *National Academy of Sciences*, 108(34), 14109-14114.
- 814 47. He, S., Barco, R. A., Emerson, D., & Roden, E. E. (2017). Comparative genomic analysis of
815 neutrophilic iron (II) oxidizer genomes for candidate genes in extracellular electron
816 transfer. *Frontiers in microbiology*, 8, 1584.
- 817 48. Hedlund, B. P., Murugapiran, S. K., Huntemann, M., Clum, A., Pillay, M., Palaniappan, K.,
818 ... & Ngan, C. Y. (2015). High-quality draft genome sequence of *Kallotenue papyrolyticum*
819 JKG1T reveals broad heterotrophic capacity focused on carbohydrate and amino acid
820 metabolism. *Genome announcements*, 3(6), e01410-15.
- 821 49. Hemp J, Ward LM, Pace LA, Fischer WW. 2015a. Draft genome sequence of *Levilinea*
822 *saccharolytica* KIBI-1, a member of the Chloroflexi class Anaerolineae. *Genome Announc*
823 3(6):e01357-15.
- 824 50. Hemp J, Ward LM, Pace LA, Fischer WW. 2015b. Draft genome sequence of *Ornatilinea*
825 *apprima* P3M-1, an anaerobic member of the Chloroflexi class Anaerolineae. *Genome*
826 *Announc* 3(6):e01353-15.
- 827 51. Hemp J, Ward LM, Pace LA, Fischer WW. 2015c. Draft genome sequence of *Ardenticatena*
828 *maritima* 110S, a thermophilic nitrate- and iron-reducing member of
829 the Chloroflexi class Ardenticatena. *Genome Announc* 3(6):e01347-15.
- 830 52. HILL, M.O., 1973, Diversity and evenness: a unifying notation and its consequences:
831 *Ecology*, v. 54, p. 427-432.
- 832 53. Hirayama, Hisako, et al. "Methylomarinovum caldicuralii gen. nov., sp. nov., a moderately
833 thermophilic methanotroph isolated from a shallow submarine hydrothermal system, and
834 proposal of the family Methylothermaceae fam. nov." *International journal of systematic and*
835 *evolutionary microbiology* 64.3 (2014): 989-999.
- 836 54. Holland HD (1984) The chemical evolution of the atmosphere and oceans. Princeton
837 University Press.
- 838 55. Hug, L. A., Baker, B. J., Anantharaman, K., Brown, C. T., Probst, A. J., Castelle, C. J., ... &
839 Suzuki, Y. (2016). A new view of the tree of life. *Nature microbiology*, 1(5), 16048.
- 840 56. Hurowitz, Joel A., et al. "Origin of acidic surface waters and the evolution of atmospheric
841 chemistry on early Mars." *Nature Geoscience* 3.5 (2010): 323-326.

- 842 57. Imhoff, Johannes F. "The Family Chromatiaceae." *The Prokaryotes*. Springer Berlin
843 Heidelberg, 2014. 151-178.
- 844 58. Inskip, W. P., Ackerman, G. G., Taylor, W. P., Kozubal, M., Korf, S., & Macur, R. E.
845 (2005). On the energetics of chemolithotrophy in nonequilibrium systems: case studies of
846 geothermal springs in Yellowstone National Park. *Geobiology*, 3(4), 297-317.
- 847 59. Johnson, J. E., Gerpheide, A., Lamb, M. P. & Fischer, W. W. O₂ constraints from
848 Paleoproterozoic detrital pyrite and uraninite. *Geol. Soc. Am. Bull.* **126**, 813–830 (2014).
- 849 60. Johnston, David T., et al. "Anoxygenic photosynthesis modulated Proterozoic oxygen and
850 sustained Earth's middle age." *Proceedings of the National Academy of Sciences* 106.40
851 (2009): 16925-16929.
- 852 61. Johnston, D. T., Poulton, S. W., Dehler, C., Porter, S., Husson, J., Canfield, D. E., & Knoll,
853 A. H. (2010). An emerging picture of Neoproterozoic ocean chemistry: Insights from the
854 Chuar Group, Grand Canyon, USA. *Earth and Planetary Science Letters*, 290(1-2), 64-73.
- 855 62. Kale, V. et al. *Litorilinea aerophila* gen. nov., sp. nov., an aerobic member of the class
856 Caldilineae, phylum Chloroflexi, isolated from an intertidal hot spring. *Int. J. Syst. Evol.*
857 *Microbiol.* 63, 1149–1154 (2013).
- 858 63. Kaneoka, Ichiro, Naoki Isshiki, and Shigeo Zashu. "K-Ar ages of the Izu-Bonin
859 islands." *Geochemical Journal* 4.2 (1970): 53-60.
- 860 64. Kang, D. D., Froula, J., Egan, R., & Wang, Z. (2015). MetaBAT, an efficient tool for
861 accurately reconstructing single genomes from complex microbial communities. *PeerJ*, 3,
862 e1165.
- 863 65. Kasting, James F. "What caused the rise of atmospheric O₂?" *Chemical Geology* 362
864 (2013): 13-25.
- 865 66. Kato, S., Kikuchi, S., Kashiwabara, T., Takahashi, Y., Suzuki, K., Itoh, T., ... & Yamagishi,
866 A. (2012). Prokaryotic abundance and community composition in a freshwater iron-rich
867 microbial mat at circumneutral pH. *Geomicrobiology Journal*, 29(10), 896-905.
- 868 67. Kato, S. et al. Comparative genomic insights into ecophysiology of neutrophilic,
869 microaerophilic iron oxidizing bacteria. *Front. Microbiol.* **6**, 1–16 (2015).
- 870 68. Katoh, Kazutaka, et al. "MAFFT: a novel method for rapid multiple sequence alignment
871 based on fast Fourier transform." *Nucleic acids research* 30.14 (2002): 3059-3066.
- 872 69. Kawaichi S, Ito N, Kamikawa R, Sugawara T, Yoshida T, Sako Y. 2013. *Ardenticatena*
873 *maritima* gen. nov., sp. nov., a ferric iron- and nitrate-reducing bacterium of the phylum
874 "Chloroflexi" isolated from an iron-rich coastal hydrothermal field, and description of
875 *Ardenticatena classis* nov. *Int J Syst Evol Microbiol* 63:2992–3002. 10.1099/ijms.0.046532-0.
- 876 70. Kawaichi, S., Yoshida, T., Sako, Y., and Nakamura, R. (2015). Draft genome sequence of a
877 heterotrophic facultative anaerobic thermophilic bacterium, *Ardenticatena maritima* strain
878 110ST. *Genome Announc.* 3:e01145-15. doi: 10.1128/genomeA.01145-15
- 879 71. Kawasumi, T., Igarashi, Y., Kodama, T., & Minoda, Y. (1980). Isolation of strictly
880 thermophilic and obligately autotrophic hydrogen bacteria. *Agricultural and Biological*
881 *Chemistry*, 44(8), 1985-1986.
- 882 72. Kharecha, P., Kasting, J. & Siefert, J. A coupled atmosphere–ecosystem model of the early
883 Archean Earth. *Geobiology* **3**, 53–76 (2005).
- 884 73. Kielak, Anna M., et al. "The ecology of Acidobacteria: moving beyond genes and
885 genomes." *Frontiers in Microbiology* 7 (2016).

- 886 74. Klatt, C. G., Bryant, D. A., & Ward, D. M. (2007). Comparative genomics provides evidence
887 for the 3-hydroxypropionate autotrophic pathway in filamentous anoxygenic phototrophic
888 bacteria and in hot spring microbial mats. *Environmental microbiology*, 9(8), 2067-2078.
- 889 75. Klatt, C. G. et al. Community ecology of hot spring cyanobacterial mats: predominant
890 populations and their functional potential. *ISME J.* 5, 1262–1278 (2011).
- 891 76. Klueglein, N., and A. Kappler. Abiotic oxidation of Fe (II) by reactive nitrogen species in
892 cultures of the nitrate-reducing Fe(II) oxidizer *Acidovorax* sp. BoFeN1—questioning the
893 existence of enzymatic Fe(II) oxidation. *Geobiology* 11.2 (2013): 180-190.
- 894 77. Konhauser, K. O. *et al.* Could bacteria have formed the Precambrian banded iron formations?
895 *Geology* **30**, 1079–1082 (2002).
- 896 78. Krepeski, S. T., Emerson, D., Hredzak-Showalter, P. L., Luther III, G. W. & Chan, C. S.
897 Morphology of biogenic iron oxides records microbial physiology and environmental
898 conditions: toward interpreting iron microfossils. *Geobiology* **11**, 457–471 (2013).
- 899 79. Kublanov, I. V., Sigalova, O. M., Gavrilov, S. N., Lebedinsky, A. V., Rinke, C., Kovaleva,
900 O., ... & Klenk, H. P. (2017). Genomic analysis of *Caldithrix abyssi*, the thermophilic
901 anaerobic bacterium of the novel bacterial phylum Calditrichaeota. *Frontiers in*
902 *microbiology*, 8, 195.
- 903 80. Kuznetsov, B. B., Ivanovsky, R. N., Keppen, O. I., Sukhacheva, M. V., Bumazhkin, B. K.,
904 Patutina, E. O., ... & Kolganova, T. V. (2011). Draft genome sequence of the anoxygenic
905 filamentous phototrophic bacterium *Oscillochloris trichoides* subsp. DG-6. *Journal of*
906 *bacteriology*, 193(1), 321-322.
- 907 81. Laslett, D., & Canback, B. (2004). ARAGORN, a program to detect tRNA genes and
908 tmRNA genes in nucleotide sequences. *Nucleic acids research*, 32(1), 11-16.
- 909 82. Lebedeva EV, Off S, Zumbragel S, Kruse M, Shagzhina A, Lucker S, Maixner F, Lipski A,
910 Daims H, Spieck E (2011) Isolation and characterization of a moderately thermophilic
911 nitrite-oxidizing bacterium from a geothermal spring. *FEMS Microbiol Ecol* 75:195–204
- 912 83. Lemoine, F., Entfellner, J. B. D., Wilkinson, E., Correia, D., Felipe, M. D., Oliveira, T., &
913 Gascuel, O. (2018). Renewing Felsenstein’s phylogenetic bootstrap in the era of big
914 data. *Nature*, 556(7702), 452.
- 915 84. Li H.*, Handsaker B.*, Wysoker A., Fennell T., Ruan J., Homer N., Marth G., Abecasis G.,
916 Durbin R. and 1000 Genome Project Data Processing Subgroup (2009) The Sequence
917 alignment/map (SAM) format and SAMtools. *Bioinformatics*, 25, 2078-9.
918 [PMID: [19505943](https://pubmed.ncbi.nlm.nih.gov/19505943/)]
- 919 85. LOZUPONE, C., AND KNIGHT, R., 2005, UniFrac: a new phylogenetic method for
920 comparing microbial communities: *Applied and Environmental Microbiology*, v. 71, p.
921 8228–8235.
- 922 86. Makita, H., Tanaka, E., Mitsunobu, S., Miyazaki, M., Nunoura, T., Uematsu, K., ... & Takai,
923 K. (2017). *Mariprofundus micogutta* sp. nov., a novel iron-oxidizing zetaproteobacterium
924 isolated from a deep-sea hydrothermal field at the Bayonnaise knoll of the Izu-Ogasawara
925 arc, and a description of *Mariprofundales* ord. nov. and *Zetaproteobacteria* classis
926 nov. *Archives of microbiology*, 199(2), 335-346.
- 927 87. Marshall, I. P., Starnawski, P., Cupit, C., Fernández Cáceres, E., Ettema, T. J., Schramm, A.,
928 & Kjeldsen, K. U. (2017). The novel bacterial phylum Calditrichaeota is diverse, widespread
929 and abundant in marine sediments and has the capacity to degrade detrital
930 proteins. *Environmental microbiology reports*, 9(4), 397-403.

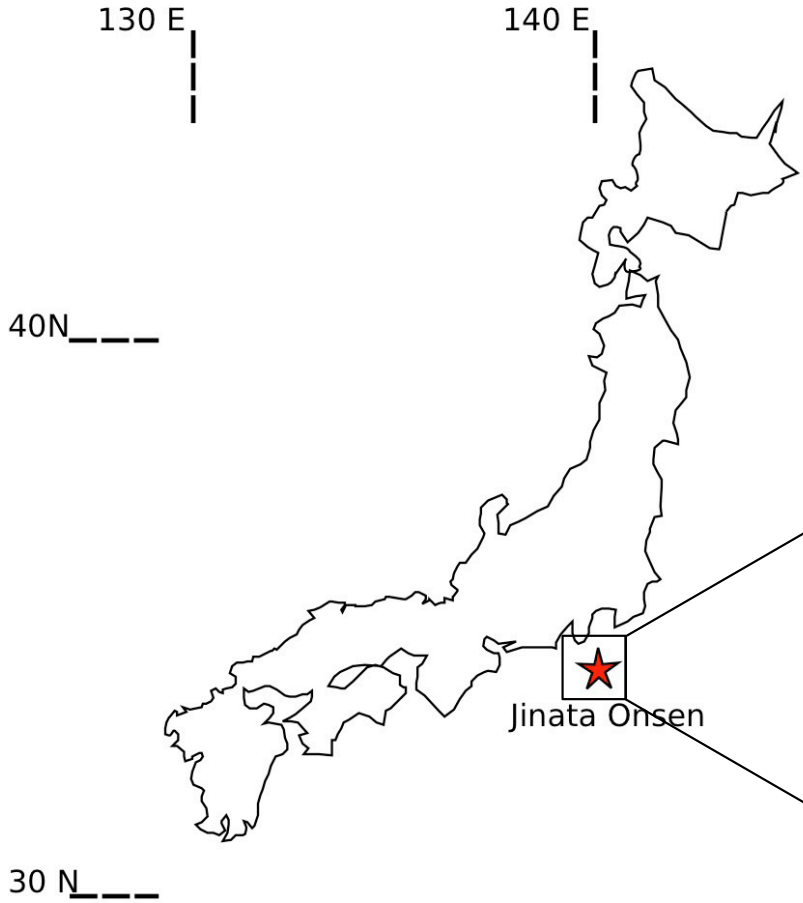
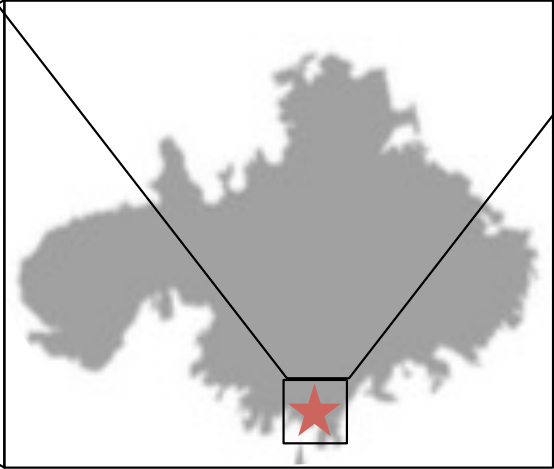
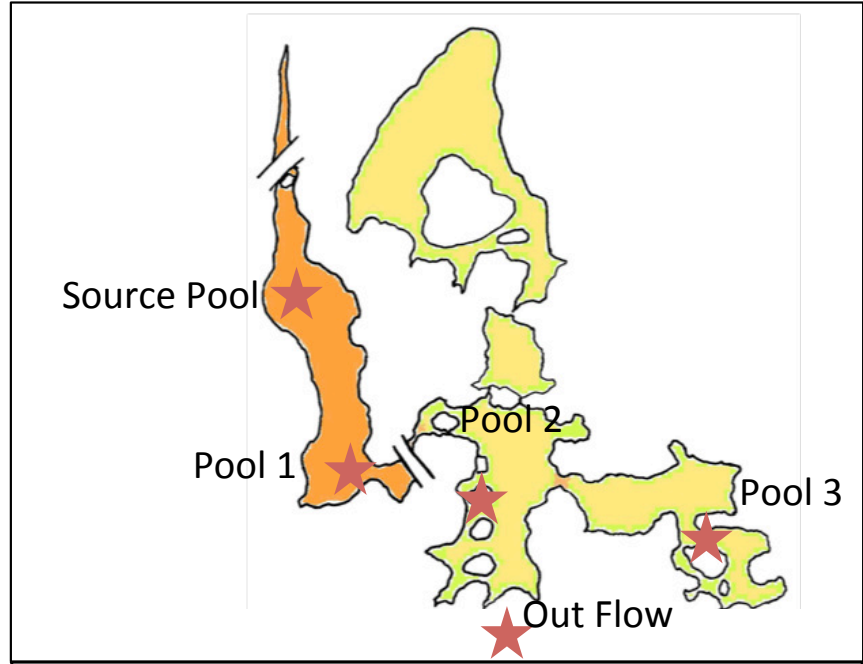
- 931 88. McIlroy, Simon Jon, and Per Halkjær Nielsen. "The family saprospiraceae." *The*
932 *Prokaryotes*. Springer Berlin Heidelberg, 2014. 863-889.
- 933 89. Meyer-Dombard, D., Jan P. Amend, and Magdalena R. Osburn. "Microbial diversity and
934 potential for arsenic and iron biogeochemical cycling at an arsenic rich, shallow-sea
935 hydrothermal vent (Tutum Bay, Papua New Guinea)." *Chemical Geology* 348 (2013): 37-47.
- 936 90. Miller, M.A., Pfeiffer, W., and Schwartz, T. (2010) "Creating the CIPRES Science Gateway
937 for inference of large phylogenetic trees" in Proceedings of the Gateway Computing
938 Environments Workshop (GCE), 14 Nov. 2010, New Orleans, LA pp 1 - 8.
- 939 91. Miroshnichenko, M. L., Kostrikina, N. A., Chernyh, N. A., Pimenov, N. V., Tourova, T. P.,
940 Antipov, A. N., et al. (2003). *Caldithrix abyssi* gen. nov., sp. nov., a nitrate-reducing,
941 thermophilic, anaerobic bacterium isolated from a Mid- Atlantic Ridge hydrothermal vent,
942 represents a novel bacterial lineage. *Int. J. Syst. Evol. Microbiol.* 53, 323–329.
- 943 92. Mori, J. F., Scott, J. J., Hager, K. W., Moyer, C. L., Küsel, K., & Emerson, D. (2017).
944 Physiological and ecological implications of an iron-or hydrogen-oxidizing member of the
945 Zetaproteobacteria, *Ghiorsea bivora*, gen. nov., sp. nov. *The ISME journal*, 11(11), 2624.
- 946 93. Neubauer, S. C. et al. Life at the energetic edge: kinetics of circumneutral Fe oxidation by
947 lithotrophic iron oxidizing bacteria isolated from the wetland plant rhizosphere. *Appl.*
948 *Environ. Microbiol.* 68, 3988–3995 (2002).
- 949 94. Oksanen, Jar, F. Guillaume Blanchet, Roeland Kindt, Pierre Legendre, Peter R. Minchin, R.
950 B. O'Hara, Gavin L. Simpson, Peter Solymos, M. Henry H. Stevens and Helene Wagner
951 (2016). *vegan: Community Ecology Package*. R package version 2.3-5. [https://CRAN.R-](https://CRAN.R-project.org/package=vegan)
952 [project.org/package=vegan](https://CRAN.R-project.org/package=vegan)
- 953 95. Pace LA, Hemp J, Ward LM, Fischer WW. 2015. Draft genome of *Thermanaerothermophilus*
954 *daxensis* GNS-1, a thermophilic facultative anaerobe from the
955 Chloroflexi class Anaerolineae. *Genome Announc* 3(6):e01354-15.
- 956 96. PARADA, A., NEEDHAM, D.M., AND FUHRMAN, J.A., 2015, Every base matters:
957 assessing small subunit rRNA primers for marine microbiomes with mock communities,
958 time-series and global field samples: *Environmental Microbiology*, v. 18, p. 1403–1414.
- 959 97. Pester, Michael, Christa Schleper, and Michael Wagner. "The Thaumarchaeota: an emerging
960 view of their phylogeny and ecophysiology." *Current opinion in microbiology* 14.3 (2011):
961 300-306.
- 962 98. Pierson, B. K., Paranteau, M. N. & Griffin, B. M. Phototrophs in high-iron- concentration
963 microbial mats: Physiological ecology of phototrophs in an iron-depositing hot spring. *Appl.*
964 *Environ. Microbiol.* 65, 5474–5483 (1999). 36.
- 965 99. Poulton, Simon W., Philip W. Fralick, and Donald E. Canfield. "Spatial variability in oceanic
966 redox structure 1.8 billion years ago." *Nature Geoscience* 3.7 (2010): 486-490.
- 967 100. Price MN, Dehal PS, Arkin AP. 2010. FastTree 2-Approximately Maximum-Likelihood
968 Trees for Large Alignments. *Plos One* 5(3).
- 969 101. Pujalte, María J., et al. "The family Rhodobacteraceae." *The Prokaryotes:*
970 *Alphaproteobacteria and Betaproteobacteria* (2014): 439-512.
- 971 102. Quast, Christian, et al. "The SILVA ribosomal RNA gene database project: improved
972 data processing and web-based tools." *Nucleic acids research* 41.D1 (2013): D590-D596.
- 973 103. R Core Team. 2014. *R: A language and environment for statistical computing*. R
974 Foundation for Statistical Computing, Vienna, Austria.

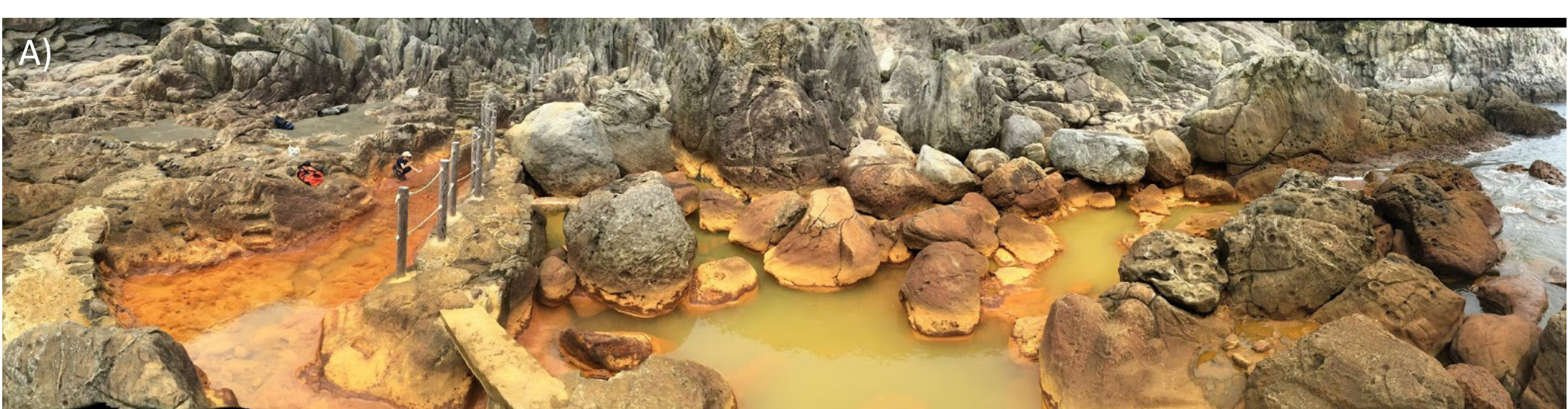
- 975 104. Rantamäki, S. et al. Oxygen produced by cyanobacteria in simulated Archean conditions
976 partly oxidizes ferrous iron but mostly escapes—conclusions about early evolution.
977 *Photosynth. Res.* 1–9 (2016).
- 978 105. Rodrigues, Jorge LM, and Jantiya Isanapong. "The family Opitutaceae." *The*
979 *Prokaryotes*. Springer Berlin Heidelberg, 2014. 751-756.
- 980 106. Roeselers, G. et al. Diversity of phototrophic bacteria in microbial mats from Arctic hot
981 springs (Greenland). *Environ. Microbiol.* 9, 26–38 (2007).
- 982 107. Rosenberg, Eugene. "The family Chitinophagaceae." *The Prokaryotes*. Springer Berlin
983 Heidelberg, 2014. 493-495.
- 984 108. Sahoo SK, et al. (2012) Ocean oxygenation in the wake of the Marinoan glaciation.
985 *Nature* 489(7417):546–549.
- 986 109. Scott, C., et al. "Tracing the stepwise oxygenation of the Proterozoic
987 ocean." *Nature* 452.7186 (2008): 456-459.
- 988 110. Sekiguchi, Y. et al. *Anaerolinea thermophila* gen. nov., sp. nov. and *Caldilinea aerophila*
989 gen. nov., sp. nov., novel filamentous thermophiles that represent a previously uncultured
990 lineage of the domain Bacteria at the subphylum level. *Int. J. Syst. Evol. Microbiol.* 53,
991 1843–1851 (2003).
- 992 111. Shannon, C. E. (1948) A mathematical theory of communication. *The Bell System*
993 *Technical Journal*, 27, 379–423 and 623–656.
- 994 112. Shih, P. M. & Matzke, N. J. Primary endosymbiosis events date to the later Proterozoic
995 with cross-calibrated phylogenetic dating of duplicated ATPase proteins. *Proc. Natl. Acad.*
996 *Sci. U. S. A.* 110, 12355–60 (2013).
- 997 113. Shih, P. M., Hemp, J., Ward, L. M., Matzke, N. J., & Fischer, W. W. (2017). Crown
998 group Oxyphotobacteria postdate the rise of oxygen. *Geobiology*, 15(1), 19-29.
- 999 114. Shih, P. M., Ward, L. M., & Fischer, W. W. (2017). Evolution of the 3-
1000 hydroxypropionate bicycle and recent transfer of anoxygenic photosynthesis into the
1001 Chloroflexi. *Proceedings of the National Academy of Sciences*, 114(40), 10749-10754.
- 1002 115. Sieber, C. M., Probst, A. J., Sharrar, A., Thomas, B. C., Hess, M., Tringe, S. G., &
1003 Banfield, J. F. (2018). Recovery of genomes from metagenomes via a dereplication,
1004 aggregation and scoring strategy. *Nature microbiology*, 1.
- 1005 116. SIMPSON, E.H., 1949, Measurement of diversity: *Nature*, v. 163, p. 688.
- 1006 117. Singer, E., Emerson, D., Webb, E. A., Barco, R. A., Kuenen, J. G., Nelson, W. C., ... &
1007 Heidelberg, J. F. (2011). *Mariprofundus ferrooxydans* PV-1 the first genome of a marine Fe
1008 (II) oxidizing Zetaproteobacterium. *PloS one*, 6(9), e25386.
- 1009 118. Skennerton, C. T. *et al.* Genomic reconstruction of an uncultured hydrothermal vent
1010 gammaproteobacterial methanotroph (family Methylothermaceae) indicates multiple
1011 adaptations to oxygen limitation. *Front. Microbiol.* 6, 1–12 (2015).
- 1012 119. Sleep, N. H., & Bird, D. K. (2007). Niches of the pre-photosynthetic biosphere and
1013 geologic preservation of Earth's earliest ecology. *Geobiology*, 5(2), 101-117.
- 1014 120. Sorokin, D. Y., Lückner, S., Vejmekova, D., Kostrikina, N. A., Kleerebezem, R., Rijpstra,
1015 W. I., et al. (2012). Nitrification expanded: discovery, physiology and genomics of a nitrite-
1016 oxidizing bacterium from the phylum Chloroflexi. *ISME J.* 6, 2245–2256. doi:
1017 10.1038/ismej.2012.70
- 1018 121. Spear, J. R., Walker, J. J., McCollom, T. M., & Pace, N. R. (2005). Hydrogen and
1019 bioenergetics in the Yellowstone geothermal ecosystem. *Proceedings of the National*
1020 *Academy of Sciences*, 102(7), 2555-2560.

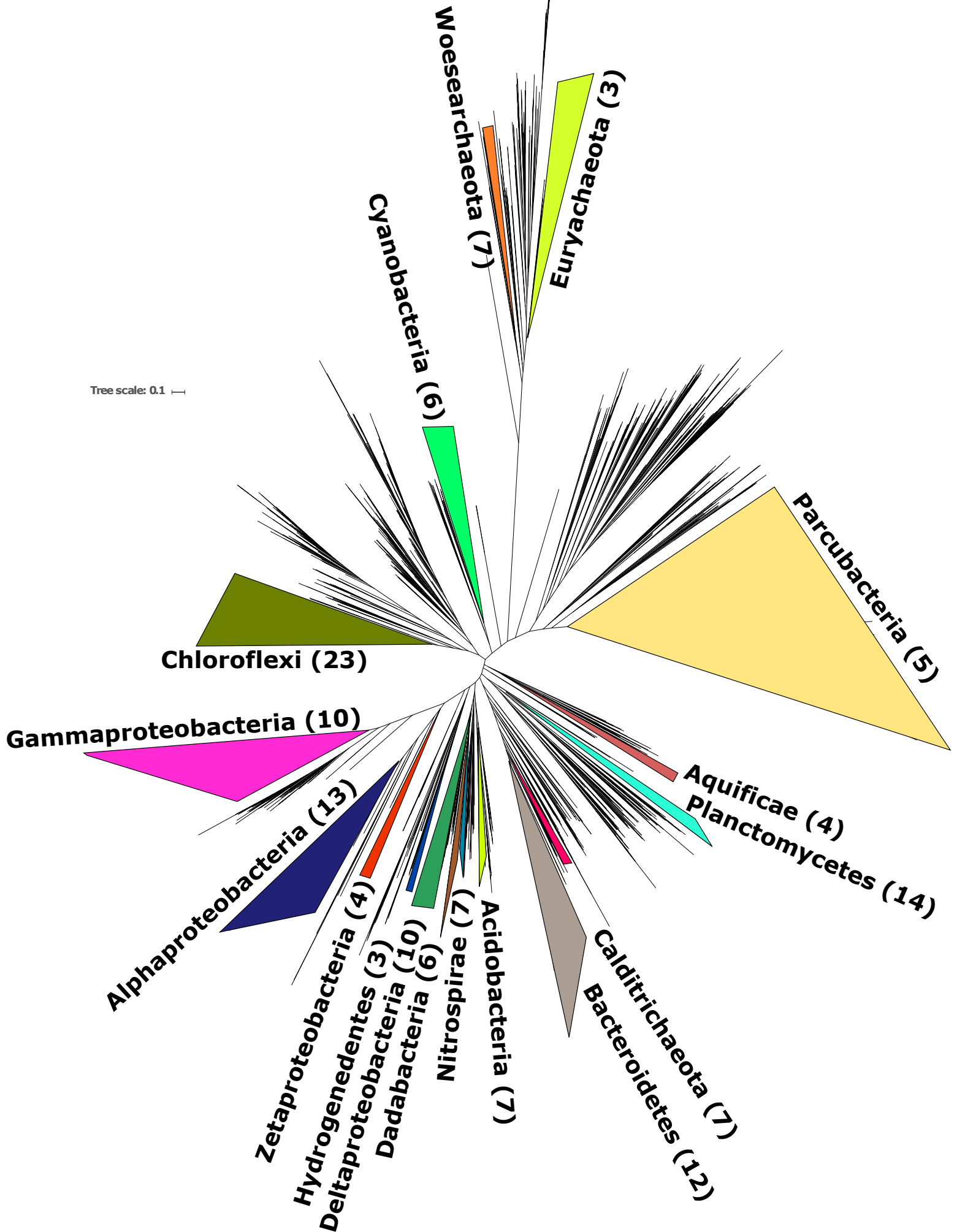
- 1021 122. A. Stamatakis: "RAxML Version 8: A tool for Phylogenetic Analysis and Post-Analysis
1022 of Large Phylogenies". Bioinformatics, 2014
- 1023 123. Stamenković V, LM Ward, M Mischna, and WW Fischer. O₂ solubility in Martian near-
1024 surface environments and implications for aerobic life. *Nature Geoscience*, in review.
- 1025 124. Stein, L. Y., & Klotz, M. G. (2016). The nitrogen cycle. *Current Biology*, 26(3), R94-
1026 R98.
- 1027 125. Stookey, Lawrence L. "Ferrozine---a new spectrophotometric reagent for
1028 iron." *Analytical chemistry* 42.7 (1970): 779-781.
- 1029 126. Strous, M., Fuerst, J. A., Kramer, E. H., Logemann, S., Muyzer, G., van de Pas-
1030 Schoonen, K. T., ... & Jetten, M. S. (1999). Missing lithotroph identified as new
1031 planctomycete. *Nature*, 400(6743), 446.
- 1032 127. Suda, K., Gilbert, A., Yamada, K., Yoshida, N., & Ueno, Y. (2017). Compound-and
1033 position-specific carbon isotopic signatures of abiogenic hydrocarbons from on-land
1034 serpentinite-hosted Hakuba Happo hot spring in Japan. *Geochimica et Cosmochimica*
1035 *Acta*, 206, 201-215.
- 1036 128. Swanner, E. D. et al. Modulation of oxygen production in Archaean oceans by episodes
1037 of Fe(II) toxicity. *Nat. Geosci.* 8, 126–130 (2015).
- 1038 129. Takai, Ken, and Satoshi Nakagawa. "The Family Hydrogenothermaceae." *The*
1039 *Prokaryotes*. Springer Berlin Heidelberg, 2014. 689-699.
- 1040 130. Takashima, C., Okumura, T., Nishida, S., Koike, H., & Kano, A. (2011). Bacterial symbiosis
1041 forming laminated iron-rich deposits in Okuokuhachikurou hot spring, Akita Prefecture,
1042 Japan. *Island Arc*, 20, 294–304.
- 1043 131. Thiel, V., Tank, M., & Bryant, D. A. (2018). Diversity of chlorophototrophic bacteria
1044 revealed in the omics era. *Annual Review of Plant Biology*, 69, 21-49.
- 1045 132. Trembath-Reichert E, Ward LM, Slotznick SP, Bachtel SL, Kerans C, Grotzinger JP,
1046 Fischer WW (2016) Gene sequencing microbial community analysis of mat morphologies,
1047 Caicos Platform, British West Indies, *Journal of Sedimentary Research* 86 (6).
- 1048 133. Trouwborst, R. E., Johnston, A., Koch, G., Luther, G. W., & Pierson, B. K. (2007).
1049 Biogeochemistry of Fe(II) oxidation in a photosynthetic microbial mat: Implications for
1050 Precambrian Fe(II) oxidation. *Geochimica et Cosmochimica Acta*, 71, 4629–4643
- 1051 134. Walker, J. C. & Brimblecombe, P. Iron and sulfur in the pre-biologic ocean. *Precambrian*
1052 *Res.* 28, 205–222 (1985).
- 1053 135. Wang Q, Garrity GM, Tiedje JM, Cole JR. 2007. Naive Bayesian classifier for rapid
1054 assignment of rRNA sequences into the new bacterial taxonomy. *Appl Environ*
1055 *Microb* 73(16): 5261-5267.
- 1056 136. Ward, L. M., Hemp, J., Pace, L. A., & Fischer, W. W. (2015a). Draft genome sequence
1057 of *Herpetosiphon geysericola* GC-42, a nonphototrophic member of the Chloroflexi class
1058 Chloroflexia. *Genome announcements*, 3(6), e01352-15.
- 1059 137. Ward LM, Hemp J, Pace LA, Fischer WW. 2015b. Draft genome sequence of *Leptolinea*
1060 *tardivitalis* YMTK-2, a mesophilic anaerobe from the Chloroflexi class Anaerolineae.
1061 *Genome Announc* 3(6):e01356-15.
- 1062 138. Ward, L. M., Kirschvink, J. L. & Fischer, W. W. 2016. Timescales of Oxygenation
1063 Following the Evolution of Oxygenic Photosynthesis. *Orig. Life Evol. Biosph.* 46(1) pp51-
1064 65.

- 1065 139. Ward, L. M. (2017). *Microbial evolution and the rise of oxygen: the roles of contingency*
1066 *and context in shaping the biosphere through time* (Doctoral dissertation, California Institute
1067 of Technology).
- 1068 140. Ward LM, A Idai, T Kakegawa, WW Fischer, and SE McGlynn. 2017a. Microbial
1069 diversity and iron oxidation at Okuoku-hachikurou Onsen, a Japanese hot spring analog of
1070 Precambrian iron formation. *Geobiology* 15 (6), 817-835.
- 1071 141. Ward, LM, SE McGlynn, and WW Fischer. 2017b. Draft genomes of a novel lineage of
1072 Armatimonadetes recovered from Japanese hot springs. *Genome Announcements*, 5:e00820-
1073 17.
- 1074 142. Ward, LM, P Shih, J Hemp, SE McGlynn, and WW Fischer. 2018a. Evolution of
1075 Phototrophy in the Chloroflexi Phylum Driven by Horizontal Gene Transfer. *Frontiers in*
1076 *Microbiology* 9, 260.
- 1077 143. Ward, L. M., Shih, P. M., and Fischer, W. W. (2018b). MetaPOAP: Presence or Absence
1078 of Metabolic Pathways in Metagenome-Assembled Genomes. *Bioinformatics*.
- 1079 144. Ward, LM, B Rasmussen, WW Fischer. 2018c. Primary Productivity was Limited by
1080 Electron Donors Prior to the Advent of Oxygenic Photosynthesis. *JGR Biogeosciences*, in
1081 review.
- 1082 145. Ward, LM, V Stamenkovic, K Hand, WW Fischer. 2018d. Follow the Oxygen:
1083 Comparative Histories of Planetary Oxygenation and Opportunities for Aerobic Life.
1084 *Astrobiology*, in review.
- 1085 146. Ward, L. M., McGlynn, S. E., & Fischer, W. W. (2018e). Draft Genome Sequence of a
1086 Divergent Anaerobic Member of the Chloroflexi Class Ardentcatenia from a Sulfidic Hot
1087 Spring. *Genome Announcements*, 6(25), e00571-18.
- 1088 147. Ward, L. M., McGlynn, S. E., & Fischer, W. W. (2018f). Draft Genome Sequences of
1089 Two Basal Members of the Anaerolineae Class of Chloroflexi from a Sulfidic Hot
1090 Spring. *Genome Announcements*, 6(25), e00570-18.
- 1091 148. Ward, LM, and PM Shih. The evolution of carbon fixation pathways in response to
1092 changes in oxygen concentration over geological time. *Free Radical Biology and Medicine*,
1093 in review.
- 1094 149. Waterhouse, A.M., Procter, J.B., Martin, D.M.A, Clamp, M. and Barton, G. J. (2009)
1095 "Jalview Version 2 - a multiple sequence alignment editor and analysis workbench"
1096 *Bioinformatics* 25 (9) 1189-1191 doi: 10.1093/bioinformatics/btp033
- 1097 150. H. Wickham. ggplot2: Elegant Graphics for Data Analysis. Springer-Verlag New York,
1098 2009.
- 1099 151. Wu, Y. W., Tang, Y. H., Tringe, S. G., Simmons, B. A., & Singer, S. W. (2014).
1100 MaxBin: an automated binning method to recover individual genomes from metagenomes
1101 using an expectation-maximization algorithm. *Microbiome*, 2(1), 26.
- 1102 152. Yamada, T. et al. Anaerolinea thermolimosa sp. nov., Levilinea saccharolytica gen. nov.,
1103 sp. nov. and Leptolinea tardivitalis gen. nov., sp. nov., novel filamentous anaerobes, and
1104 description of the new classes Anaerolineae classis nov. and Caldilineae classis nov. in the.
1105 *Int. J. Syst. Evol. Microbiol.* 56, 1331–1340 (2006).
- 1106 153. Yamada, T., & Sekiguchi, Y. (2009). Cultivation of uncultured chloroflexi subphyla:
1107 significance and ecophysiology of formerly uncultured chloroflexi subphylum i'with natural
1108 and biotechnological relevance. *Microbes and Environments*, 24(3), 205-216.

- 1109 154. Yoon, J., Jang, J. H. & Kasai, H. *Algisphaera agarilytica* gen nov, sp nov, a novel
1110 representative of the class Phycisphaerae within the phylum Planctomycetes isolated from a
1111 marine alga. *Antonie van Leeuwenhoek, Int. J. Gen. Mol. Microbiol.* **105**, 317–324 (2014)
1112 155. Youssef, N. H. *et al.* In Silico Analysis of the Metabolic Potential and Niche
1113 Specialization of Candidate Phylum ‘Latescibacteria’ (WS3). *PLoS One* **10**, e0127499
1114 (2015).
1115 156. Zerkle, A. L. *et al.* Onset of the aerobic nitrogen cycle during the Great Oxidation Event.
1116 *Nature* 1–10 (2017). doi:10.1038/nature20826







Tree scale: 0.1

